9-27-2010

Macrophage Integrin-Mediated, HuR-Dependent Angiogenic Factor Gene Expression

Yasha Modi

Macrophage Integrin-Mediated, HuR-Dependent Angiogenic Factor Gene Expression

A Thesis Submitted to the
Yale University School of Medicine
In Partial Fulfillment of the Requirements for the
Degree of Doctor of Medicine

Yasha S. Modi
2009

Macrophage Integrin-Mediated, HuR-Dependent Angiogenic Factor Gene Expression

Yasha Modi, Jiange Zhang, Timur Yarovinsky, Mark Collinge, Gautham K. Rao, Yizhun Zhu, Jeffrey R. Bender, Yale University, New Haven, CT.

Activated macrophages, via the secretion of pro-angiogenic factors, modulate the angiogenic response to inflammation. Several of these factors, including vascular endothelial growth factor (VEGF), are encoded by inherently unstable mRNA transcripts containing AU-rich elements (AREs) in their 3' untranslated region. During stress events, the half-lives of these mRNAs must be prolonged to allow for significant protein production and an adequate angiogenic response. This laboratory has demonstrated that engagement of the β2-integrin receptor, LFA-1, leads to stabilization of ARE-bearing mRNAs in T lymphocytes through a nuclear-to-cytoplasmic translocation of the RNA-binding protein, HuR. Here, we address whether β2-integrin engagement stabilizes VEGF mRNA in macrophages *in vitro* and at sites of angiogenesis via a HuR-dependent mechanism.

To determine whether β2-integrin engagement regulates VEGF mRNA stability, we adhered primary mouse bone marrow-derived macrophages to ICAM-1 (β2-integrin ligand) for 3 hours. VEGF mRNA degradation was measured by quantitative RT-PCR after transcriptional inhibition. In the cells bound to ICAM-1, the VEGF mRNA remained stable, whereas, in non-integrin engaged control cells, VEGF mRNA degraded to less than 50% of initial levels within 60 minutes. Furthermore, in BMDMs deficient in HuR expression, VEGF mRNA from integrin-engaged cells degraded to 50% within 60 minutes, thus supporting the essential role of HuR in this stabilization event.

To study inflammatory angiogenesis *in vivo*, we used a subcutaneous polyvinyl alcohol (PVA) sponge model to assess differences in wild-type and "macrophage-specific" conditional HuR knockout ($HuR^{flox/flox}$LysM-Cre) mice. Flow cytometry analyses of cells extracted from PVA sponges at 1 to 4 weeks showed equal recruitment of $F4/80^{+}$ cells in wild-type and HuR knockout mice. Immunofluorescence staining of excised PVA sponges confirmed equal macrophage recruitment and localization but revealed a reduction of VEGF production. Preliminary results indicate that formation of $CD31^{+}$ microvessels in HuR knockout mice is also decreased.

We conclude that macrophage β2-integrin engagement results in stabilization of VEGF and that expression of HuR in macrophages is required for neovascular responses. These findings are relevant to understanding the post-transcriptional regulatory mechanisms of inflammatory angiogenesis.

Acknowledgements

I would like to thank Dr. Bender for his assistance and mentorship since the summer of 2006. He has provided insightful comments and suggestions to enhance my experience as a researcher. Furthermore, he has been encouraging and supportive of all my career aspirations and decisions. This year would not have been possible without Dr. Bender's unwavering support—he has significantly enhanced my experience as a researcher and medical student and I cannot thank him enough.

I would like to thank Dr. Timur Yarovinsky, a senior researcher in the lab, who has played an integral role in my development as a researcher this past year. His patient guidance has undoubtedly improved my approach to developing and carrying out a hypothesis-driven experiment.

I would like to thank Gautham Rao, a postdoctoral fellow in the lab, who has always been available to answer my questions and guide my research. Also, I would like to thank Jian-ge Zhang who graciously collaborated with me on ongoing projects. Together, we approached related questions from different angles, producing synergistic results.

I would like to thank Mark Collinge, a former senior researcher, who not only introduced me to the technical components of research, but inspired me to pursue a one-year fellowship in the same laboratory.

I would like to thank Dr. Themis Kyriakides for showing our lab how to implement the PVA sponge implant model. I would like to thank Maya Kotas, a M.D./Ph.D. student, for showing our lab how to isolate and culture bone marrow derived macrophages.

This project was funded by the Howard Hughes Medical Institute one-year Medical Fellows Program and the National Institute of Health RO1HL61782 grant.

Table of Contents

***Introduction*:**

The process of small blood vessel formation in adults is called neovascularization or angiogenesis. This process occurs from pre-existing vessels or from the recruitment of endothelial progenitor cells (EPCs) from the bone marrow into tissues. Angiogenesis, responding to a complex set of stimuli, occurs in both physiologic and pathologic conditions. Embryogenesis and remodeling of the capillary bed in adult skeletal muscle in response to regular exercise are examples of the former (1). Pathologic conditions that induce angiogenesis include tumor growth, ischemic injury, and chronic inflammation. In the setting of cardiovascular disease, such as coronary artery disease, there are components of both ischemia and inflammation that promote angiogenesis. It has been previously shown that the extent of coronary artery collateral circulation (angiogenic-induced circulation) is the primary determinant of the extent of necrosis (2). This collateral development was shown to be mediated by angiogenic growth factors (3, 4), such as vascular endothelial growth factor (VEGF) and basic fibroblast growth factor (b-FGF) in response to inflammatory and ischemic stimuli (5, 6, 7). Numerous growth factors and cell types have since been identified to contribute to the complex regulation of this phenomenon.

VEGF is one of the most extensively studied angiogenic growth factors. Seven VEGF isoforms (VEGF-A, VEGF-B, VEGF-C, VEGF-D, VEGF-E, VEGF-F and placental growth factor) are formed as a result of alternative splicing from a single VEGF gene. In humans, the abundant isoforms include $VEGF_{121}$, $VEGF_{165}$, $VEGF_{189}$, and $VEGF_{206}$, which differ in their molecular mass and in their biological properties, such as their heparin-binding affinity. VEGF serves as an endothelial cell mitogen stimulating

proliferation, migration and tube formation that is necessary for the development of neovessels (8). This activity is essential during embryogenesis. The deletion of one VEGF allele arrests angiogenesis resulting in embryonic lethality (9). Furthermore, dysregulation of VEGF results in tumor angiogenesis (10) and retinal disease (11).

The expression of VEGF is upregulated in response to hypoxia, oncogenes, and several cytokines (12). Hypoxia has been the best studied stimulus to VEGF gene expression with several identified mechanisms (13). Potentiation occurs via increased transcription, mRNA stability, and at the level of protein translation. The increase in VEGF transcription is mainly regulated through the hypoxia inducible factor-1 (HIF-1). HIF-1 is a transcription factor consisting of two subunits. HIF-1α serves as the inducible component while HIF-1β is constitutively produced (14). Under physiologic conditions, HIF-1α remains inactive via targeting through proteosomal degradation by hydroxylation. Under hypoxic conditions, the hydroxylation event is inhibited resulting in salvage of the HIF-1α subunit. This subunits complexes with the HIF-1β subunit, translocates into the nucleus and binds to the hypoxia responsive element (HRE) in the 5' region of the VEGF gene allowing for transcriptional upregulation (15, 16, 17).

At the level of mRNA stability, *in vitro* mRNA degradation assays in cell lines have confirmed that the VEGF mRNA half life is 60 minutes under normoxic conditions. However, under hypoxic conditions, the half-life of VEGF mRNA increases by 2-3 fold (7). This mechanism of stability is due to the a RNA-binding protein, HuR, which binds to the 3' untranslated region (UTR) of the VEGF mRNA, protecting it from degradation by endonucleases (18, 19). This method of regulation is the focus of this study and will be discussed in greater detail below.

Control at the level of protein translation is believed to occur via regulation of the VEGF mRNA transcript at the internal ribosomal entry site (IRES) as well as by increased expression of oxygen-regulated protein 150 (ORP 150). The 5' UTR of VEGF mRNA contains many IRES, which are sites of attachment for the ribosome. These sites are thought to provide alternative sites for translational control for VEGF (20).

ORP 150 is believed to be an alternative site for translational control. This protein is a chaperone required for transport of proteins from the endoplasmic reticulum to the golgi apparatus. This protein is upregulated in response to hypoxia, which is believed to result in increased VEGF protein transport and secretion (21).

These mechanisms of VEGF gene expression regulation allude to the complex role of angiogenic regulation in response to stressors, such as hypoxia. This regulation occurs in a number of cells that participate in the angiogenic response. Several studies have identified macrophages as one of the key cell types in regulating the angiogenic response. Macrophages, playing a large role in innate immune protection, are involved in anti-bacterial or anti-tumor activity (phagocytosis), antigen presentation, and the production and release of a variety of regulatory factors including peptides (cytokines), prostanoids, and enzymes (22, 23). Macrophages originate from bone marrow progenitors (i.e. monoblasts, promonocytes) and circulate as monocytes (24, 25). Under physiologic conditions, monocytes circulate in the blood with a 3 day half-life in humans (26). Under pathologic conditions, there is a significant increase in bone marrow production, a shorter circulation time, and increased tissue extravasation, causing macrophage accumulation at pathologic tissue sites (27). In fact, almost any disturbance in the local milieu, including infection, wound healing, ischemia, malignancy, immune

activation, or normal cell turnover results in recruitment of macrophages to the area (28). This recruitment from the blood stream to sites of injury is generically referred to as "macrophage activation".

It has been well documented that activated macrophages play a role in modulating the angiogenic response (29), particularly via the secretion of angiogenic factors, including VEGF, tumor necrosis factor α (TNF-α), monocyte chemoattract protein 1 (MCP-1), and granulocyte-macrophage colony-stimulating-factor (GM-CSF). Chemokines secreted during the ischemic response (by resident macrophages and other inflammatory cell types) recruit monocytes to the affected region, where these monocytes adhere to the endothelium, transmigrate into the ischemic tissue, differentiate into macrophages and produce VEGF and other pro-angiogenic substances upon activation.

The recruitment to sites of inflammation or ischemia is a key component of macrophage activation. Monocyte adhesion receptors engage endothelium adhesion ligands. Leukocyte glycoproteins, called selectins, allow for reversible cell binding on endothelium by engaging oligosaccharide ligands on the endothelium (30, 31). This interaction is not strong enough to anchor the cells against the force of blood flow, which leads to a series of engagement/ disengagement events that allow the leukocyte to roll on the endothelium. Furthermore, this engagement is not cytokine driven.

Integrins are adhesion receptors which allow for tighter binding. The two most studied macrophage integrins are the β2-integrins, Mac-1 (also known as CR3) and lymphocyte function-associated antigen-1 (LFA-1). LFA-1, a αLβ2 integrin, is a heterodimeric protein consisting of the subunits CD11a and CD18 (30). As monocytes approach the hypoxic tissue under the influence of chemokines, LFA-1, which is

expressed on the plasma membranes of monocytes, macrophages, and lymphocytes, engages its ligand, the intercellular adhesion molecules (ICAMs). This group of ligands or counter-receptors, consisting mostly of ICAM-1 and ICAM-2, are proteins within the immunoglobulin superfamily that are expressed by APCs as well as vascular endothelium (31, 32). This engagement not only allows for strong adhesion and transmigration of the leukocyte through the endothelium, but also results in LFA-1 activation (33, 34). The transmembrane signaling cascade that ensues includes multiple second messenger and kinase activation events, including inositol phosphate (IP3) (35, 36), phospholipase C (PLC) (37) and protein kinase C (38).

In the activated state, after chemokine induction and LFA-1 engagement, macrophages produce several pro-inflammatory and pro-angiogenic cytokines, which have tightly controlled expression profiles. As previously mentioned, these pro-angiogenic mRNAs are inherently unstable, but upon activation, the half lives of the transcripts are increased resulting in greater protein production (39). This suggests a significant posttranscriptional regulatory mechanism for cytokine production. At rest, the degradation process of these transcripts is rapidly initiated by shortening of the 3' poly (A) tails (40). The unifying component of these short-lived cytokines is that the mRNAs possess a conserved adenine and uridine (AU)-rich element (ARE) in their 3' untranslated region (UTR), which makes them highly susceptible to rapid degradation by RNAases after transcription (40). Two studies have identified a specific nonameric sequence (UUAUUUAUU) responsible for this destabilization (41, 42). Several regulatory proteins have high binding affinities to RNAs containing these AREs, which further regulate the half lives of these transcripts. Some ARE-binding proteins

destabilize the transcripts. Examples include AU-rich element RNA-binding protein 1 (AUF1) (43) and KH-type splicing regulatory protein (KSRP) (44). Some ARE-binding proteins, however, stabilize the transcript. One such protein, HuR, is a member of the Hu family of RNA binding proteins. This protein is a nucleocytoplasmic protein, located almost exclusively in the nucleus under rest conditions, but translocates into the cytoplasm after cellular activation (45). Previous studies have shown that HuR binds to AREs and stabilizes cytokine transcripts, allowing for greater protein production (46). Specific to angiogenic transcripts, the Levy groups has shown in a rat myocyte cell line that HuR binds the AREs in the 3' UTR of VEGF mRNAs, increasing the half-life of the transcript 2-3 fold (7). Thus, mRNA stabilization is a crucial regulatory process that determines the overall production of cytokine and angiogenic substances.

The connection between HuR and the transmembrane signals induced by β2 integrin LFA-1 engagement are of particular importance in understanding mRNA stabilization. Previous results in T lymphocytes from the Bender lab have shown that engagement of LFA-1 in human peripheral T cells significantly extends the half-life of ARE-containing transcripts, including TNF-α, GM-CSM, and Interleukin 3 (IL-3), with consequent enhanced protein production. Furthermore, LFA-1 engagement is necessary for the nuclear-to-cytoplasmic translocation of the mRNA-stabilizing protein, HuR. This redistributed cytoplasmic HuR is capable of binding an AU-rich element sequence in vitro. Finally, abrogation of HuR levels by use of inhibitory peptides or RNA interference prevents LFA-1 engagement-mediated stabilization of these mRNA transcripts in T cells (46). Taken together, these results clearly demonstrate the

connection between LFA-1 engagement and HuR-mediated mRNA stabilization in T cells.

We hypothesize that the interaction between LFA-1 and HuR is similar in the macrophage. Once in the cytoplasm, HuR can bind to the ARE sequence of an angiogenic mRNA transcript, providing the necessary stability to facilitate angiogenic factor production. Although never studied in the macrophage, the Levy group has previously shown in various cell lines that HuR modulates VEGF mRNA stability. However, the role of integrin engagement controlling HuR modulation has never been investigated. It is our intention to study this connection in the macrophage using VEGF transcript stability as one of our representative markers for posttranscriptional angiogenic regulation.

There is little known about the mechanisms regulating angiogenic factor mRNA stabilization *in vivo*, and how those mechanisms play roles in dynamic responses to ischemia and inflammation. In particular, how chemokine stimulated monocyte recruitment and β2 integrin-mediated cell adhesion/transmigration enhance early neovascular responses to tissue ischemia, through effects on mRNA stability, is a truly novel aspect of vascular biology and physiology. This has great relevance in the context of both peripheral and coronary artery disease, in which ischemic skeletal or cardiac muscle often remains viable only if there are prominent angiogenic responses.

***Hypothesis*:**

In response to chronic inflammation or tissue ischemia, monocyte/macrophage β2 integrin engagement results in modulation of the mRNA-binding protein HuR, resulting in stabilization of VEGF transcripts and enhanced angiogenic responses. Macrophage-specific HuR gene deletion results in a diminished angiogenic response.

***Specific Aims*:**

1. To determine whether β2-integrin-induced VEGF mRNA stabilization is HuR dependent in murine bone marrow derived macrophages (BMDMs).
2. To determine whether β2-integrin-induced VEGF mRNA stabilization is lost in macrophages obtained from HuR knockout mice.
3. To use the macrophage-specific HuR knockout mice in *in vivo* angiogenesis assays using a sponge implantation model.

***Methods*:**

(All work was performed by Yasha S. Modi unless stated otherwise)

Antibodies and Reagents

The following antibodies were used: anti-HuR (3A2) antibody (Santa Cruz, Ca), anti-p38MAPK (Cell Signaling, MA), phospho-p38MAPK (Cell signaling, MA) FITC-conjugated anti-F4/80 (eBioscience, CA), Alexa 648-conjugated anti-F4/80 (eBioscience, CA), PE-conjugated anti-CD11b (BD Pharmingen, NJ), anti-CD31 (PECAM (BD Pharmingen, NJ), cyanine-3-conjugated goat anti-mouse antibody (Jackson Immunoresearch, PA), and IRDye 800 conjugated goat anti-rabbit (Rockland, PA). Other agents included 5,6-dichloro-1-β-D-ribobenzimidazole (DRB) (Sigma, MO) and DAPI (Sigma, MO).

The constituents of "LFA-1 activation buffer" include: 100 mM Tris. HCL, pH 7.4, 150 mM NaCl, 2 mM $MnCl_2$, 20 mM $MgCl_2$, D-glucose 5 mM, and 1.5 % BSA. The constituents of "fully supplemented" RPMI media include: 10% fetal bovine serum, 2 mM glutamine, 25 mM HEPES, 1.75 µL 2-Mercaptoethanol**,** 1 mM Sodium Pyruvate**,** and 100 U/ml each of penicillin G and streptomycin. "L Cell supernatant" is supernatant from "fully supplemented media" 12 days after plating (10 days post confluence) of L929 cells, a fibroblast tumor line. 2:1 RPMI:L Cell or "macrophage growth media" signifies two parts fully supplemented RPMI and 1 part L Cell supernatant.

Bone Marrow Extraction and Macrophage Isolation

Macrophages were extracted and cultured from C57BL/6 wild type ($HuR^{flox/flox}$) or macrophage-specific HuR knockout mice ($HuR^{flox/flox}$lysMcre). Mice were first anesthetized by placement into an isoflurane chamber and euthanized by cervical

dislocation. Femurs and tibias were isolated, washed (1x 70% ethanol, 3x in CMF-PBS), and ground with a mortar and pestle in fully-supplemented RPMI media. Bone homogenate was then filtered through a 70 µm filter and centrifuged at 1500 RPM at room temperature. Cells were resuspended in RBC lysis buffer (0.15 mM NH_4CL, 1 mM $KHCO_3$, 0.1 mM EDTA) in order to lyse red blood cells. Cells were then washed once, counted, and plated in "macrophage-growth media" at a concentration of 4 million cells/7 mL media in a 10 cm non-tissue culture petri dish. Cells were left in this media for 7 days, with addition of 4 ml fresh media on day 4 (47). The "macrophage-growth media" consists of monocyte colony stimulating factor (M-CSF) enriched media + fully supplemented RPMI in a 1:2 ratio. M-CSF enriched media was generated by collection of supernatant from a fibroblast tumor line 10 days after confluence was achieved (L929 cell line, "L cell media").

VEGF mRNA Decay Assay

Petri dishes were coated with 100ng/ml recombinant murine ICAM-1/Fc chimera protein (R&D Systems**,** MN) in 2% dialyzed FBS/CMF-PBS overnight at 4˚C. Control plates were coated with an Fc conjugate, Goat-α-Human IgG, Fc fragment (Jackson Immunoresearch, PA), and blocked overnight in 2% dialyzed FBS/CMF-PBS at 4˚C. Murine bone-marrow derived macrophages ($4x10^6$/sample) in "LFA-1 activation buffer" were allowed to adhere to ICAM-1 coated plates or the Fc conjugate control plates. "LFA-1 activation buffer" (100 mM Tris. HCL, pH 7.4, 150 mM NaCl, 2 mM $MnCl_2$, 20 mM $MgCl_2$, D-glucose 5 mM, and 1.5 % BSA) is a cation-based solution that allows cations, particularly manganese, to bind to the metal ion-dependent adhesion site (MIDAS) on the ligand-binding domain of LFA-1 (48). This binding induces an

allosteric transition to a high affinity state for its ligand (ICAM-1, in this experiment), aiding in cell adhesion without cell activation. After 30 minutes of cell adhesion, the activation buffer was aspirated and replaced with fully supplemented RPMI for 2.5 hours. mRNA synthesis was inhibited after a total of 3 hrs incubation (0.5 hrs in activation buffer, 2.5 hours in RPMI) by the addition of 25 μM of the RNA polymerase II inhibitor 5,6-dichloro-1-β-D-ribobenzimidazole (DRB) (Sigma, MO). Non-adherent cells were aspirated and adherent cells were lysed in RLT lysis buffer (Qiagen, Ca) containing β-mercaptoethanol (2-ME) at various time points post DRB addition for RNA isolation. RNA was isolated with the Qiagen RNeasy kit (Qiagen, Ca). cDNA was generated from 1 μg of total RNA with iScript (Bio-rad, CA). Analysis was performed via quantitative real-time PCR (Opticon 2 sytem, MJ Research, MA) using a SYBR Green PCR kit (Qiagen, Ca). Murine VEGF mRNA levels were normalized against beta-actin with expression levels relative to time 0 when transcription was inhibited. The sequence of the VEGF primers used for RT-PCR was: Forward primer: GGAGATCCTTCGAGGAGCACTT, Reverse primer: GGCGATTTAGCAGCAGATATAAGAA. The sequence of the housekeeping beta actin primers used for RT-PCR was: Forward primer: GTGGGCCGCTCTAGGCACCAA, Reverse primer: TGGCTTTAGGGTTCAGGGGG. The primers were designed by Gautham Rao and synthesized by the Keck Biotechnology resource facility at Yale.

HuR Translocation and Immunofluorescence

Sterile glass coverslips were coated with 100ng/ml murine ICAM-1/Fc chimera protein in 2% dialyzed FBS/CMF-PBS overnight at 4˚C. Control coverslips were coated with an Fc conjugate (Goat-α-Human IgG, Fc fragment) and blocked overnight in 2%

dialyzed FBS/CMF-PBS at 4˚C. Murine bone-marrow derived macrophages (10^6/sample), in "LFA-1 activation buffer" were allowed to adhere to ICAM-1 coated plates or the Fc conjugate control plates for 45 minutes. Cells were then fixed with 4% paraformaldehyde and permeabilized with 0.1 % triton X-100. Cells were blocked with 5% goat serum for 2 hours at room temperature and then incubated in anti-HuR antibody (1:500) overnight at 4˚C. Cells were then washed and incubated with cyanine 3-conjugated goat anti-mouse antibody (1:1000) for 1 hour at room temperature. Cells were then counterstained with 0.005 % 4',6-diamidino-2-phenylindole (DAPI) for nuclear staining.

p38MAPK Phosphorylation Assay

Petri dishes were coated with 100ng/ml murine ICAM-1/Fc chimera protein in 2% dialyzed FBS/CMF-PBS overnight at 4˚C. Control plates were coated with an Fc conjugate (Goat-α-Human IgG, Fc fragment). Murine bone-marrow derived macrophages ($4x10^6$/sample), in "LFA-1 activation buffer" were allowed to adhere to ICAM-1 coated plates or the Fc conjugate control plates for 5, 10, 15, and 20 minutes. Cells were subsequently lysed in RIPA cell lysis buffer (1% Sodium Deoxycholate, 0.1% SDS, 1% NP-40, and protease inhibitor in PBS). Total protein was run on a 10% SDS-PAGE gel, transferred to nitrocellulose membrane, and immunoblotted with anti-phospho-p38MAPK (1:1000), and anti-p38MAPK (1:1000, loading control). Of note, it is accepted practice to quantitatively measure p38 activation with antibodies against phosphorylated p38 MAPK. After 3x washing, the membrane was probed with IRDye conjugated goat-anti-rabbit (1:10000) and visualized using an Odyssey Imaging System (LI-COR Biosciences, Nebraska).

Overview of Development of $HuR^{flox/flox}$LysMcre Mouse (Macrophage-Specific HuR Knockout Out)

The development of the $HuR^{flox/flox}$LysMcre started in 2004 and was designed and developed by Mark Collinge, a former senior researcher in the Bender laboratory. All genetic modifications were performed on a C57BL/6 background. Briefly, exon 2 of the HuR gene was targeted and via standard gene targeting (49, 50), the gene was floxed by "loxP" cre recombinase recognition sites. By crossing mice, both alleles of the HuR gene were floxed, providing the designation $HuR^{flox/flox}$. Confirmation of homozygous floxing was determined by genotype analysis. This mouse was then crossed with a genetically engineered mouse expressing cre recombinase under the control of the LysM promoter (Jackson Laboratories, ME). The LysM promoter is found exclusively in macrophages and neutrophils, and thus the LysM driven cre recombination only results in HuR excision in macrophages and neutrophils. After multiple generations of crossing, the lab generated a $HuR^{flox/flox}$LysMcre mouse. This mouse was genotypically confirmed to be homozygous for LysM cre expression. Of note, the acquired mouse expressing cre recombinase, has the recombinase gene genetically targeted in place of the lysozyme M gene. That is, the $HuR^{flox/flox}$LysMcre is in fact a double knockout in macrophages and neutrophils, deficient in HuR and LysM cre. This decision was consciously made as lysozyme M does not play a known role in inflammatory and ischemia-induced angiogenesis.

Surgical Model of Chronic Inflammation: Polyvinyl Alcohol Sponge Implantation & Harvesting

Implantation: Polyvinyl Alcohol (PVA) Sponges (Ultracell Medical Technologies, Inc., CT) were cut into 1mm x 2mm sections in a sterile fashion. Mice were anesthetized using 10% ketamine (stock: 100 mg/mL), 5% xylazine (stock: 20 mg/mL) saline based solution. The dorsum of the animal was shaved and cleaned with iodine/alcohol. A 1.25 cm incision was made along the spine from mid-back to upper back. The skin was retracted and lateral blunt dissections were made subcutaneously 1.5 cm away from the incision site to create right and left subcutaneous pockets. A sponge section (1 mm x 2 mm) was inserted into each subcutaneous pocket and the skin was stapled shut for 1 week.

Explantation: Mice with PVA sponge implants were euthanized and the dorsum overlaying the implant site was shaved. The original incisions were reopened and sponges were extracted along with adherent skin to preserve orientation. For immunohistochemistry, sponges with adherent skin were fixed in a formalin-free zinc fixative solution (BD Pharmingen, NJ), embedded in paraffin, and sectioned into 5 µm sections. Paraffin embedding and sectioning was performed by the Yale Pathology Department. Immunohistochemistry staining using anti-CD31 antibody (1:50) was performed (secondary antibody: biotinylated anti-rat, Vector Labs, California). For RNA isolation, sponges without adherent skin were homogenized using a tissue homogenizer in lysis buffer. For flow cytometry, sponges without adherent skin were minced using a razor blade and cells were extracted by type I collagenase (274 U/ml) (Worthington, NJ) treatment. RBCs were subsequently lysed using the RBC lysis buffer (described above).

Microarray Analysis:

The microarray analysis was developed to assess gene expression profile differences between WT and KO bone marrow derived macrophages (BMDMs) adhered and non-adhered to ICAM-1. Groups included "WT No Treatment", "HuR KO No Treatment", "WT ICAM", "KO ICAM", where "WT" denotes BMDM from $HuR^{flox/flox}$ mice and "KO" denotes $HuR^{flox/flox}$LysMcre mice. Furthermore "No Treatment" implies cells harvested and not adhered, while "ICAM" denotes macrophages bound to ICAM-1 (LFA-1 engaged).

Bone marrow derived macrophages (BMDMs) from $HuR^{flox/flox}$ (WT) mice and $HuR^{flox/flox}$LysMcre (KO) mice were cultured in triplicate (3 WT mice, 3 KO mice on different days) in order to account for biological variability. The "no treatment" control samples were pooled from the three independent WT and KO macrophage cultures upon harvesting, comprising the "WT No Treatment" and "KO No Treatment" categories, respectively. After compiling the total macrophages from each sample, there were a total of 5 million cells for the "WT No Treatment" group and "KO No Treatment group" (1.67 million BMDMs from each WT and KO culture x 3 cultures).

To determine the effect of macrophage adhesion to ICAM-1, *the following experiment was repeated 3 times in identical fashion on sequential days*: Petri dishes were coated with 100ng/ml murine ICAM-1/Fc chimera protein in 2% dialyzed FBS/CMF-PBS overnight at 4˚C. Control plates were coated with an Fc conjugate (Goat-α-Human IgG, Fc fragment) and blocked overnight in 2% dialyzed FBS/CMF-PBS at 4˚C. Murine BMDMs ($5x10^6$/sample) in "LFA-1 activation buffer" were allowed to adhere to ICAM-1 coated plates or the Fc conjugate control plates. After 30 minutes of cell adhesion, the activation buffer was aspirated and replaced with fully supplemented

RPMI for 2.5 hours. At three hours, non-adherent cells were aspirated and adherent cells were lysed (in RLT lysis buffer + 2-ME) for RNA isolation. RNA was isolated with the Qiagen RNeasy kit. Subsequent RNA samples were sent to the Keck Biotechnology resource facility at Yale. A total of 8 samples were given to them for hybridization: Compiled "WT No Treatment", compiled "KO No Treatment", 3 "WT ICAM" samples, and 3 "KO ICAM" samples.

All subsequent steps to analysis were performed by the Keck Biotechnology facility. Briefly, these steps involve converting total RNA to amplified, labeled cRNA prior to hybridization. First, the total RNA is reverse transcribed to cDNA via use of the poly (A) RNA present. Single stranded cDNA is then converted into double stranded cDNA and purified (Illumina TotalPrep RNA Amplification Kit, CA). This is followed by an overnight *in vitro* transcription (IVT) reaction in the presence of biotinylated UTP and CTP to generate biotin-labeled cRNA. The cRNA then undergoes a purification step using the same Amplification Kit. 1.5 µg of cRNA from each sample (8 total samples) is then hybridized to the MouseRef-8 v1.1 Expression BeadChip (Illumina, CA).

***Results*:**

Bone marrow extraction yields a 93 to 98.5% pure population of F4/80+, CD11b+ cells.

Prior to performing *in vitro* studies with cultured BMDMs, it was important to check the efficiency and purity of BMDM cultured via our isolation technique. From C57BL/6 mice, tibias and femurs were isolated. Bone marrow cells were extracted and cultured in "macrophage growth media" for 7 days. On day 7, the non-adherent cells were removed and the adherent cells were collected for analysis. Cells were double stained for F4/80 (FITC) and CD11b (PE), two standard macrophage markers. The results are illustrated in Figure 1. After gating on the live population of cells, 94% of the cells are double positive, indicating 6% non-macrophage cells. Similar experiments confirmed 93.5 to 98.4% double-positive macrophages (data not shown). These results demonstrate that the macrophage isolation, differentiation, and expansion protocol is yielding relatively pure numbers of macrophages.

LFA-1 engagement induces VEGF mRNA stabilization

Previous studies from the Bender lab have demonstrated the role of LFA-1 engagement-mediated mRNA stabilization after engagement to ICAM-1, a physiologic ligand of LFA-1, in T cells. As macrophages play a large role in the angiogenic response, our first aim was to assess whether LFA-1 engagement promotes VEGF mRNA stabilization. BMDMs were harvested at day 7 of differentiation and were used to perform an *in vitro* mRNA decay assay (as described in the "Methods" section). To measure the half life of BMDM transcripts present at the time of transcriptional arrest, adherent cells were lysed at 0, 30, and 60 minutes post DRB (RNA polymerase II

inhibitor) addition. The transcript levels of VEGF were compared to the stable, housekeeping mRNA encoding beta actin at each time point. The results are illustrated in Figure 2. The x-axis represents time after DRB addition while the y-axis demonstrates normalized VEGF mRNA as a % of time 0 (DRB addition). When BMDMs are not LFA-1 engaged (plated on Fc control plates), their VEGF mRNA transcripts decays to 50 % (t ½) within 30 minutes. However, when macrophages are bound to ICAM-1 (LFA-1 engaged), their transcript levels remain constant through 60 minutes post-transcriptional arrest. These results demonstrate that LFA-1 engagement by ICAM-1 leads to stabilization of the mRNA transcript encoding the pro-angiogenic cytokine, VEGF.

LFA-1 engagement results in HuR nuclear-to-cytoplasmic translocation

VEGF mRNA transcripts contain destabilizing AREs in their 3'-UTRs (7). Since HuR has been shown to bind mRNA AREs and prevent degradation of those transcripts, and since LFA-1 engagement induces VEGF transcript stability, we hypothesized that LFA-1 engagement stabilizes transcripts via HuR. Previous studies from the Bender lab have shown that LFA-1 engagement results in HuR nuclear-to-cytoplasmic translocation and subsequent mRNA binding to class II AREs in T cells (46). Here we assess whether LFA-1 engagement causes HuR translocation in murine BMDMs. Mature murine BMDMs underwent 45 minutes of an *in vitro* translocation assay (see "Methods" section), then were fixed, permeablized and stained with anti-HuR antibody (with DAPI counter-stain for nuclear definition). Immunofluorescence images are depicted in Figure 3. After 45 minutes of adhesion to ICAM-1, a substantial amount of HuR has translocated out of the nucleus, seen clearly in the overlay image. In the presence of LFA-1 activation buffer with cells adhered to control coverslips (Fc conjugate antibody),

HuR remains exclusively nuclear. This demonstrates that BMDM LFA-1 engagement results in HuR nuclear-to-cytoplasmic translocation, which is consistent with the hypothesis that LFA-1 engagement stabilizes transcripts via HuR.

Macrophage LFA-1 engagement activates the p38 MAPK pathway

After demonstrating with murine BMDMs that LFA-1 engagement results in HuR translocation and stabilization of VEGF mRNA transcripts, we sought to define the signaling molecules in this rapid, posttranslational event. Previous data from the Bender lab in T cells has shown that LFA-1 engagement with resultant HuR translocation is mediated via Rho family GTPase Rac (Rac 1 and Rac 2). p38 MAPK is a downstream Rac effector that has been linked to modulation of mRNA stability. Here we demonstrate the activation of p38 MAPK after LFA-1 engagement in murine BMDMs. Mature macrophages were used for an *in vitro* p38 MAPK phosphorylation assay (see "Methods" section). Time points were 5, 10, 15, and 20 minutes. An immunoblot was prepared and probed for activation-specific p38 phosphorylation. Loading controls were determined by probing for total p38. The immunoblot is shown in Figure 4. Within 5 minutes of BMDM engagement to ICAM-1, there is a substantial induction (greater than 6-fold) of phosphorylation (activation), which persists throughout the 25 minute time course. Preliminary experiments have recently shown that the p38 inhibitor SB203580 blocks adhesion-induced mRNA stabilization (not shown). Together, these data demonstrate that LFA-1 stimulated p38 activation is required for induced mRNA stabilization.

The HuR$^{flox/flox}$LysMcre (HuR, macrophage specific knockout) mouse yields inconsistent knockdown of HuR

The $HuR^{flox/flox}$LysMcre mouse was developed by a senior researcher (Mark Collinge) in the Bender laboratory (Figure 5). Briefly, exon 2 of the HuR gene was genetically targeted by "loxP" cre recombinase recognition sites, producing a homozygous (both alleles "floxed") $HuR^{flox/flox}$ mouse. This mouse was subsequently crossed with a genetically engineered mouse expressing cre recombinase under the control of the LysM promoter. The LysM promoter is active exclusively in macrophages and neutrophils, and thus the LysM promoter driven Cre recombination event results in HuR excision only in macrophages and neutrophils. The immunoblot in figure 6 confirms the specificity of the $HuR^{flox/flox}$LysMcre knockout mouse (figure courtesy of Mark Collinge). In immunoblot A, HuR is absent in the $HuR^{flox/flox}$LysMcre bone-marrow derived macrophages (KO) but present in the $HuR^{flox/flox}$ macrophages (WT). When isolating the splenic lymphocytes (immunoblot B) from the same mice, it is evident that the HuR levels are present and equal. Additional immunoblots using extracts from BMDMs isolated from different mice were performed. Figure 7 illustrates the variable knockdown of HuR protein levels in BMDMs from 3 WT and 3 KO mice. Comparing WT 1 vs. KO 1, the knockdown of HuR is approximately 95%. However, when comparing WT 2 vs. KO 2, the knockdown of HuR is approximately 53%. This variability in knockdown using the lysozyme M promoter in a cre-lox system has been previously described (51). This particular study, using the LysMcre system for cell-specific conditional knockdown has demonstrated a deletion efficiency of 83-98% in mature macrophages. The knockdown efficiency in neutrophils in that study was significantly greater, approaching 100%. The variability in our system is greater than has been previously described (53-95% in our knockdown versus 83-98% in the Clausen

group knockdown). Similar variation can be observed when assessing the transcript levels of HuR (Figure 8). To ensure the biological variability inherent to the system, technical errors in genotyping were ruled out and all mice were re-confirmed to have the $HuR^{flox/flox}$ (WT) and $HuR^{flox/flox}$LysMcre (KO) genotype. Reasons for the potential variability in HuR excision may include insufficient or untimely expression of Cre recombinase. Little is known about the control of the Lysozyme M promoter which is driving cre recombinase expression. Alternatively, there may be inadequate excision at the loxP recognition sites. Chromatin structure may prevent the cre recombinase from recognizing or binding to the loxP sites, resulting in incomplete excision. Finally, as the BMDM colonies in which these cells are taken from are 93-98% pure macrophages, the other cells (non-macrophages but expressing HuR) may explain the variable levels of HuR present within the immunoblot. Further analysis is underway to identify the significant variability in the LysMcre system.

FACS analysis of bone-marrow derived macrophages and monocytes confirms a variable knockdown of HuR in the $HuR^{flox/flox}$LysMcre mouse

To determine whether HuR found in $HuR^{flox/flox}$LysMcre cells is expressed in macrophages or contaminating cells, we used intracellular staining for HuR followed by FACS analysis. BMDMs were harvested on day 7 after culture in macrophage growth media. In order to acquire peripheral blood monocytes, peripheral blood was drawn from WT and KO mice via retrobulbar bleeding. BMDMs and monocytes were surface co-stained with Alexa 647-conjugated F4/80 (1:200) and PE-conjugated CD11b (1:400). Intracellular HuR staining was achieved by permeabilizing the cells in a 0.2% saponin wash and staining with Anti-HuR (3A2) antibody conjugated to a zenon alexa 488 tag

(Invitrogen). Single color controls and isotype controls to anti-HuR antibody (mouse IgG1 isotype control) were also prepared. HuR expression levels from WT and KO BMDMs are illustrated in Figure 9. After double-gating for CD11b+, F4/80+ cells, HuR expression levels (via a histogram) may be assessed on the macrophage population. The shift in the WT HuR stained curve compared to the KO HuR stained curve illustrates differential expression levels of HuR. As the KO curve almost overlaps the isotype control, it is apparent that the majority (but not all) of HuR is absent. Complete knockdown would be represented by absolute overlap of the KO stained curve with the isotype curve. In order to confirm the presence of HuR in the CD11b+, F4/80+ cell population, a technique of "back-gating" was used. When gating only the HuR positive cells from the KO sample (difference between KO HuR and KO isotype histogram), a small percentage of these HuR gated cells are CD11b+, F4/80+ macrophages (Figure 10). This result provides further evidence that $HuR^{flox/flox}$LysMcre (KO) macrophages are expressing low levels of HuR. That is, the impurity of the BMDM cultures (2-7% non-macrophages) cannot fully explain the variable levels of HuR expression in the $HuR^{flox/flox}$LysMcre macrophages.

HuR expression levels from WT and KO blood monocytes are illustrated in Figure 11. As described above, after double-gating for CD11b+, F4/80+ cells, HuR expression levels may be assessed on the monocyte population. Compared to BMDMs, the shift in the WT HuR-positive curve relative to the isotype control is substantially smaller. This may be the result of incomplete staining or may indicate that blood monocytes express less HuR than BMDMs. Furthermore, blood monocytes from $HuR^{flox/flox}$LysMcre (KO) mice showed more residual HuR. This recapitulates the

question of variable and insufficient cre recombinase expression under the control of the LysM promoter. Although unproven, it is possible that differentiation from monocyte to activated macrophage may alter the activity of the LysM promoter along with cre recombinase expression. Of note, when assessing HuR levels in the CD11b+, F4/80- quadrant, which is representative of granulocytes (and NK cells), the expression of HuR from the KO mouse is almost completely absent (overlaps the isotype control). This is consistent with the findings of the Forster group who described the efficiency of deletion in neutrophils approaching 100% (51).

After discovering that both BMDMs and monocytes from the $HuR^{flox/flox}$LysMcre mouse had variable levels of HuR expression, prior screening was required for all subsequent experiments to establish the level of knockdown. For all *in vitro* experiments, mature BMDMs were screened via intracellular HuR staining and assessed by FACS to ensure at least 90% knockdown. If knockdown was less efficient than this, the cells were not used for experimentation. For all *in vivo* experiments, blood monocytes (acquired via retrobulbar bleed) were screened via intracellular HuR staining and assessed by FACS to ensure at least 75% knockdown. Mice were allowed to reconstitute their cell counts after bleeding for one week prior to surgical implantation/manipulation. The threshold for acceptance was lower when assessing blood monocytes to account for incomplete intracellular HuR staining.

LFA-1 engagement induces VEGF mRNA stabilization in WT but not in KO BMDMs

As described above, LFA-1 engagement by ICAM-1 leads to stabilization of mRNA transcripts encoding the pro-angiogenic cytokine, VEGF. The mechanism of

LFA-1 engagement resulting in VEGF mRNA stabilization is believed to be HuR-dependent. In order to confirm this hypothesis, an identical *in vitro* mRNA stabilization assay was performed using BMDMs from $HuR^{flox/flox}$LysMcre (KO) mice and $HuR^{flox/flox}$ (WT) mice. The results are illustrated in Figure 12. Consistent with previous results, LFA-1 engaged BMDMs from WT mice demonstrated stability of the VEGF mRNA transcript through 60 minutes post-transcription arrest. However, VEGF mRNA transcripts from LFA-1 engaged KO BMDMs decayed to its half life by 60 minutes. These results indeed demonstrate that VEGF mRNA stabilization after β2 integrin engagement is HuR-dependent.

LFA-1-induced VEGF protein levels is decreased in KO macrophages.

After establishing the necessity of HuR for VEGF mRNA stability and confirming the labile nature of KO VEGF mRNA transcripts in BMDMs, we hypothesized that VEGF protein levels would be greater in WT macrophages compared to KO macrophages after LFA-1 engagement (as a direct result of increased mRNA stability). WT and KO BMDMs in LFA-1 activation buffer were adhered to ICAM-1-coated or Fc conjugate-coated plates for 30 minutes, then cultured in fully supplemented RPMI media (without L Cell supplementation) for an additional 23.5 hours. After 24 hours, supernatant was collected for evaluation of VEGF protein levels and the adherent cells were collected to confirm at least 90% knockdown of HuR protein expression via western blot (figure not shown). VEGF ELISA results are illustrated in Figure 13. There is a modest increase (~30%) in VEGF protein obtained from ICAM-bound WT BMDM supernatants, relative to the non-integrin engaged control (WT ICAM vs. WT NO ICAM). This integrin-induced augmentation in VEGF protein secretion is lost in the KO

BMDMs (KO ICAM vs. KO NO ICAM). Furthermore, there is a large reduction in baseline VEGF secretion in the KO cells (WT NO ICAM vs. KO NO ICAM), demonstrating the role for HuR in both basal and integrin-induced VEGF production. This is not surprising given the documented importance of HuR in VEGF mRNA stability.

Polyvinyl Alcohol (PVA) sponge implants from HuR$^{flox/flox}$LysMcre (KO) mice have substantially decreased levels of VEGF mRNA at 2 weeks post-implantation.

In vitro BMDM data confirmed that LFA-1 engagement results in VEGF mRNA stabilization. Via the use of HuR$^{flox/flox}$LysMcre (KO) mouse macrophages, this stabilization was determined to be HuR-dependent. To assess the importance of this phenomenon, an *in vivo* model of chronic inflammation was used. The polyvinyl alcohol sponge implantation model was used because it induces a well-established chronic inflammatory response comprised of significant macrophage recruitment and obvious angiogenesis (52). Approximately 60% of the cells isolated from a sponge after 6 weeks (via FACS analysis) are macrophages (F4/80+, CD11b+) (figure not shown). Furthermore, recruitment of macrophages to sites of inflammation requires LFA-1 engagement. Of note, several presumptions were made regarding this surgical model. First, the cells infiltrating the sponges are mostly macrophages that have been LFA-1 engaged and activated. Second, the neovascularization event is driven by macrophages and is VEGF-dependent.

Sterile PVA sponges were placed in surgically constructed subcutaneous pockets into the dorsum of the WT and KO mice. At various time points (3 days, 1, 2, 3, and 4 weeks), the mice were euthanized and the sponges were explanted. For RNA isolation,

the skin was detached from the sponge. Murine VEGF mRNA levels were normalized against beta actin. The results are illustrated in Figure 14. The VEGF mRNA levels obtained from sponges implanted in WT mice were nine-fold greater than that obtained from sponges implanted in KO mice at 2 weeks. This trend persisted through 3 and 4 weeks but was not as dramatic due to significantly decreased VEGF mRNA expression after 2 weeks. These results provide the first evidence that differences in WT and KO VEGF mRNA, likely the result of impaired mRNA stabilization in HuR-deficient macrophages, can be recapitulated *in vivo*.

Recruitment of F4/80+, CD11B+ macrophages to the PVA sponge in WT and KO mice are identical.

Before drawing conclusions about reduced KO macrophage VEGF production in this model, it was important to determine equal macrophage localization in sponges implanted in WT and KO mice. That is, any differences in VEGF levels or consequent angiogenesis must be attributed to a defect in macrophage factor production, and not attributed to varying levels of macrophages within the sponge. The critical time points for assessing macrophage recruitment were chosen to correspond to maximal VEGF production and neovascularization (2, 3, and 4 week post-implantation). As described above, PVA sponges were implanted subcutaneously over the dorsum of WT and KO mice. Sponges were explanted at 2, 3, and 4 weeks post-implantation and cells were extracted via Collagenase Type I digestion. RBCs were subsequently lysed and cells were double stained for FACS analysis with murine alexa-647 conjugated anti-F4/80 antibody and murine PE-conjugated anti-CD11b antibody. Figure 15 illustrates equal macrophage recruitment from sponges implanted in WT and KO mice at 3 and 4 weeks.

Similar results were obtained at 2 weeks (figure not shown). Based on cell counts before FACs staining, absolute numbers of F4/80+, CD11b+ cells can be generated, with approximately 5 x 10^5 macrophages obtained from 3 week sponges and 3.5-4 x 10^5 macrophages from 4 week sponges. These findings indicate that the varying levels of VEGF mRNA are not due to differences in macrophage recruitment. Rather, these differences are due to biologic differences between WT and KO recruited cells.

There is only a modest reduction of CD31+ vessels in sponges from KO mice compared to sponges from WT mice.

After observing significant differences in VEGF expression levels between the WT and KO mouse at 2, 3, and 4 weeks post-implantation, it was hypothesized that there would be decreased neovessels in the KO mouse compared to the WT mouse. Sponges and adherent skin were explanted at 2, 3, and 4 weeks post-implantation and fixed, paraffin embedded and sectioned. PECAM (CD31) immunohistochemical staining was performed (Figure 16). The arrows indicate sponge neovessel. The quantified results for 2 week and 4 week WT and KO sponges are illustrated in Figure 17A. The results for a repeat experiment on 3 week and 4 week WT and KO sponges are illustrated in Figure 17B. All vessels were manually counted by two people who were blinded to the sample. The first figure represents an average number of CD31+ vessels in 25 fields of view under high magnification, while the second analysis represents all the CD31+ vessels present in each sponge. Numbers represent an average of the two counts. Taken together, these results indicate that there is a reduction in neovessel formation at 3 and 4 weeks in the KO-mouse derived sponges compared to the sponges from the WT mouse but that the reduction is only modest.

300 genes are upregulated in both WT and KO BMDMs upon adhesion to ICAM-1

The microarray analysis was the first discovery study by our lab looking to assess gene expression differences between WT and KO BMDMs adhered and non-adhered to ICAM-1. Groups included "WT No Treatment", "HuR KO No Treatment", "WT ICAM", "KO ICAM", where "WT" denotes BMDM from $HuR^{fl/fl}$ mice and "KO" denotes $HuR^{fl/fl}$LysMcre mice. Furthermore, "No Treatment" denotes cells harvested and not adhered, while "ICAM" denotes macrophages bound to ICAM-1. Time of adhesion was arbitrarily chosen as 3 hours. With these four conditions, three key questions may be answered. First, expression profiles upon engagement to ICAM-1 may be assessed; this is a HuR independent finding and would not vary between WT and KO BMDMs. Second, comparing the unbound ("No Tx") WT and KO BMDMs, baseline (un-adhered) expression profile differences that are dependent on HuR levels may be assessed. Finally, using all four conditions, expression profile differences may be determined that are both ICAM dependent (increased /decreased expression on adherence to ICAM-1) *and* HuR dependent (increased/decreased expression in BMDMS from KO mice). Staying consistent with our hypothesis that ICAM-1 adherence leads to a stabilization of transcripts (therefore higher mRNA levels) and that HuR is required for this stabilization, our analysis focused mainly on genes upregulated after adhesion to ICAM-1 and on genes downregulated in BMDMs acquired from KO mice.

After completion of the microarray experiment, a total of 8 RNA samples were given to the Keck biotechnology facility for microarray hybridization: Compiled "WT No Treatment", compiled "KO No Treatment", 3 "WT ICAM" samples, and 3 "KO ICAM" samples. All analysis was performed using the Beadstudio data analysis software

(Illumina, CA). The first analysis compared genes with statistically significant differences between ICAM-bound versus non-ICAM bound samples, using WT No TX as the reference group. That is, all listed genes show a significant induction on ICAM over untreated samples. Statistical significance was determined by use of a "differential (Diff) score". The Diff score is a log transformation of the *p*-value. The formula is: Diffscore = 10 x sgn(μref-μcond) x log10(*p*). The translation is as follows: for a *p*-value of 0.05, the Diff Score = ± 13, for a *p*-value of 0.01, the Diff Score = ±20, for a *p*-value of 0.001, the Diff Score = ± 30. This transformation is useful because it provides directionality to the *p*-value based on the difference between the average signal in the reference group (WT No Tx in this analysis) vs. the comparison group. This study utilized a Diff score of +/- 13 to establish significance. In order to identify genes that have LFA-1 dependent (bound to ICAM-1) gene expression profiles, an "AND/OR tree" was used to filter genes that conform to this profile. With the reference group set to "Wt No Tx", branch 1 of the tree was as follows: KO, diff score > 13, KO, diff score <-13. Branch 2 was: KO, *p*-value < 0.01, WT No Tx, *p*-value < 0.01. This filter produced 5924 genes, of which 300 genes had positive Diff scores greater than or equal to 13 comparing WT ICAM bound to the reference group. That is, there was a significant induction on ICAM relative to the "WT No Tx" sample. Of these genes, several chemokine genes had significant induction patterns on ICAM-1. These chemokines were selected for validation via RT-PCR. Primers were designed for CCL2, CCL3, CCL4, CCL5, and CCL7. An identical experiment was conducted using BMDMs from a WT and KO mouse. The results are illustrated in Figure 18. For all chemokines analyzed, there was a significant induction on ICAM-1 relative to the "WT No Tx" group. The

patterns of gene expression between WT ICAM and KO ICAM were equal or only slightly varied, however, suggesting HuR independence.

The second analysis was designed to assess genes with statistically significant differences between the bound "WT ICAM" and "KO ICAM" samples. This study was designed to address not only the HuR dependent genes, but also the HuR *and* LFA-1 dependent genes. The reference group was set to "KO 3 ICAM". The "KO ICAM" groups were run in triplicate and this sample had the largest knockdown of HuR expression levels (90%) on retrospective analysis via RT-PCR. Once again, Diff scores of +/- 13 were set as our cutoff for achieving statistical significance. In order to identify genes that are HuR dependent, an "AND/OR tree" was used to filter genes that conform to this profile. An "AND/OR tree" was developed. Branch 1: WT 3, diff score > 13, WT 3, diff score <-13, and Branch 2: WT 3 detection p value < .01, KO 3 detection p value < .01. The total number of genes displayed that fit this filter was 1045. When assessing genes with + diff scores of 13 or more (significant induction on WT ICAM 3 or KO ICAM 3), 29 genes fit this pattern (Table). That is, there is a HuR dependent component to each of these genes. Furthermore, 5 of these genes appear to be both dependent on HuR and induced on ICAM-1. These genes are Caveolin 1 (Cav 1), TAP Binding Protein (TAPBP), Moesin (Msn), G protein-coupled receptor 84 (GPR84), and RNA binding protein gene with multiple splicing (RBPMS) (Figure 19). Interestingly, none of the inflammatory or angiogenic cytokines that are known to be HuR-dependent (i.e. TNF-α) appeared on this list. As for the five genes that have emerged from this list, the connection between HuR or LFA-1 has not been made. Furthermore, these findings are currently being validated to confirm both HuR and LFA-1 dependence.

Discussion:

Our results support the hypothesis that monocyte/macrophage β2 integrin engagement results in modulation of the mRNA-binding protein HuR, resulting in stabilization of VEGF mRNA. *In vitro* experiments demonstrate that bone-marrow derived macrophage LFA-1 engagement results in stabilization of otherwise labile VEGF mRNA transcripts. HuR-deficient BMDMs lose integrin VEGF mRNA stabilization. These results are consistent with previous findings by the Bender laboratory which showed that human peripheral T cell LFA-1 engagement significantly extends the half-lives of ARE-containing transcripts, including TNF-α, GM-CSF, and IL-3 (46).

The molecular signaling pathway responsible for transducing the signal between LFA-1 engagement and HuR nuclear-to-cytoplasmic translocation in BMDMs remains unknown. This study suggests that p38 is in the pathway. Previous work done in our lab on peripheral human T cells demonstrates that LFA-1 activates Vav-1 in a PI-3 kinase dependent manner. Vav-1 is a guanine nucleotide exchange factor (GEF) for Rac-1 and Rac-2, both members of the Rho family of GTPases. Activation of Vav-1 causes the Rac molecules to exchange its GDP for GTP, activating Rac and thus its downstream effectors. Both Vav-1 and Rac activation are required for T cell LFA-1 mediated mRNA stabilization (Ramgolam, manuscript submitted). We propose that p38 is the critical downstream Rac effector leading to HuR translocation and labile mRNA stabilization. Although we assume that the proximal, required signaling molecules are identical in T cells and macrophages, this may not be correct. For example, macrophages may have different GEFs, required for GTP loading of Racs. Studies are ongoing in our laboratory to define any macrophage-specific components of this pathway.

The role of HuR in conferring stability to ARE-bearing transcripts (i.e. VEGF mRNA) in BMDMs remains to be fully understood. Demonstrating VEGF mRNA stabilization and HuR translocation after LFA-1 engagement suggests that HuR plays a role in integrin-induced posttranscriptional regulation of VEGF mRNA. However, to confirm this, a macrophage-specific HuR knockout mouse was generated by a senior researcher (Mark Collinge) in our laboratory. This mouse, described in the methods sections, involves *in vivo* gene targeting, engineering "loxP" cre recombinase recognition sites flanking exon 2 of the HuR gene. This mouse was then crossed with a transgenically engineered mouse expressing cre recombinase under the control of the Lysozyme M promoter. After several breeding generations, a $HuR^{flox/flox}$LysMcre mouse was generated. This mouse, via western blot analysis, was confirmed to be a tissue-specific knockdown. That is, the mouse was partially deficient in HuR in macrophages and neutrophils, but not in other cell types. However, the knockdown efficiency was determined to be variable and sometimes incomplete. Analysis of three random $HuR^{flox/flox}$LysMcre (KO) mice showed that HuR knockdown varied significantly (from 53-95% knockdown). The variability in knockdown using the lysozyme M promoter has been previously described (51), with a reported deletion efficiency of 83-98% in mature macrophages. The variability in our system is significantly greater than that reported by Clausen et al. As mentioned above, there may be variability in the level of cre recombinase expression. That is, cre recombinase is under the control of the Lysozyme M promoter—little is known about the regulation of this promoter. Alternatively, for a multitude of reasons, there may be inadequate excision of exon 2 at the loxP recognition

sites. Reasons for this are diverse spanning from poor binding (i.e. inaccessible chromatin structure) to insufficient cre recombinase protein.

In subsequent experiments, BMDMs from $HuR^{flox/flox}$LysMcre mice were screened for a minimum HuR knockdown efficiency of 90%. This value was arbitrarily set to include only our best knockdowns in experimentation. Thus, when repeating the mRNA stabilization assay using knockout macrophages, we were able to show that BMDMs with a 90% knockdown of HuR showed a loss of VEGF mRNA stability after LFA-1engagement. These results confirmed our initial hypothesis that LFA-1-induced stabilization of VEGF mRNA is HuR-dependent. Interestingly, VEGF mRNA transcripts from WT non-LFA-1 engaged cells from the previous experiment (Figure 2) decayed to their half-life by 30 minutes while VEGF mRNA transcripts from KO LFA-1 engaged cells decayed to their half–life by 60 minutes (Figure 12). That is, with less than 10% of the original HuR protein expression, there was still a partial stabilizing effect on VEGF mRNA, yielding a half-life that was twice as long as non-LFA-1 engaged cells.

When corresponding this to the protein level, an interesting result surfaced which suggested that both basal and stimulated (integrin-activated) VEGF protein expression is dependent on HuR. We have not investigated the HuR-dependent augmentation of basal VEGF levels in these cells, which retain HuR in the nucleus in non-activated cells.

Although these findings are focused around LFA-1 engaged VEGF mRNA stability, the extrapolation could be made to all pro-angiogenic factors containing AREs in the 3' UTR region of the mRNA transcript. That is, HuR might stabilize and prolong the half-lives of several pro-angiogenic transcripts containing AREs. Preliminary results from the Bender laboratory have shown that BMDM LFA-1 engagement confers both

Matrix Metallopeptidase 9 (MMP9) and Angiopoietin 2 mRNA stability. MMP9 participates in extracellular breakdown during angiogenesis (allowing for endothelial migration) and tissue remodeling (54). Angiopoietin 2 has been implicated in tube formation, migration of endothelial cells, vessel sprouting and regression during an angiogenic response (55). Both possess AREs in their 3'UTR which make them amenable to stabilization by HuR.

After confirming an essential role for HuR in the posttranscriptional regulation of the pro-angiogenic cytokines *in vitro*, we assessed whether these results could be replicated *in vivo*. VEGF has been shown to play a critical role in regulating inflammatory and ischemic angiogenesis *in vivo* (56). Therefore, the development of a macrophage-driven model involving inflammatory angiogenesis was implemented. Polyvinyl Alcohol (PVA) sponges were implanted subcutaneously to induce a chronic inflammatory process. Two assumptions were made prior to proceeding. Cells infiltrating the sponges are mostly macrophages that have been LFA-1 engaged and activated. Secondly, the neovascularization event is driven by macrophages and is VEGF dependent. Analysis was conducted at 2-4 weeks to assess VEGF levels along with corresponding vascularity. At 2 weeks, there was a large induction of VEGF mRNA in the sponges from WT mice compared to that in the sponges from KO mice. This trend persisted through 4 weeks but was less apparent as the levels of VEGF mRNA precipitously declined after 2 weeks. The number of macrophages infiltrating the sponge were assessed and shown to be equal in both the KO and WT mice. This confirms that the KO mouse did not have a leukocyte recruitment defect. All differences in VEGF mRNA levels, therefore, were directly attributable to the differential expression and

regulation of the macrophages rather than the number of macrophages present. Finally, when assessing vascularity via CD31+ staining on paraffin-embedded sections of the sponge, there appeared to be no difference at 2 weeks, and a modest reduction of blood vessels in sponges from the KO mouse at 3 and 4 weeks.

Despite significant variation in the level of VEGF mRNA expression, the KO mouse had a minimally different angiogenic phenotype from the WT mouse. There are several possible explanations for this. First, the macrophage-specific HuR knockout mouse yields an incomplete knockdown. It is unclear exactly how much HuR is required to result in stabilization. At 90% knockdown in our *in vitro* studies, there were noticeable differences in VEGF mRNA stability. However, despite 90% knockdown, the half life of the VEGF mRNA transcript was twice as long (60 minutes) when compared to non-LFA-1 engaged WT samples (30 minutes) indicating some stabilization. When screening the KO mice for this particular experiment, blood monocytes were assessed via FACs analysis and determined to be at least 75% HuR depleted. This lower criterion was established to account for incomplete staining via the intracellular HuR staining method currently in place. Assuming such a low threshold during screening of the mice, and showing in our *in vitro* studies that less than 10% HuR within a cell has some stabilizing effect, the mice used for this *in vivo* study might have sufficient levels of HuR to differentially stabilize alternative angiogenic transcripts. That is, although there was a large difference in VEGF mRNA stability, perhaps other ARE-bearing angiogenic transcripts may have been stabilized in the KO mouse, minimizing the angiogenic phenotype of this mouse.

Furthermore, in our *in vivo* model, there may be several non-HuR dependent angiogenic factors contributing to the angiogenic phenotype, thus masking the contribution of HuR dependent angiogenic factors. There may also be alternative cell types, such as fibrocytes that contribute to the angiogenic phenotype in a model of chronic inflammation. Fibrocytes are connective tissue fibroblast-like cells that circulate through the peripheral blood (57). After subcutaneous implantation of "wound chambers" in mice, they are rapidly recruited to the site of inflammation where they proliferate. In this inflammatory milieu, fibrocytes produce and secrete MMP-9, VEGF, basic fibroblast growth factor (bFGF), IL-8, and platelet derived growth factor (PDGF) which together, promote endothelial cell migration, proliferation, and tube formation (58). These are the same pro-angiogenic transcripts that are produced by macrophages. In our model, fibrocytes should have normal HuR levels. Thus, these fibrocytes may mask the macrophage-dependent angiogenic component that was originally in question.

To counter some of these concerns, an alternative model of ischemic angiogenesis is currently being implemented in the Bender laboratory. This model involves hindlimb ligation of the femoral artery to induce a stable but severe ischemic hindlimb (59). This model was implemented under similar assumptions from the sponge implant. That is, cells infiltrating the ischemic muscle are mostly macrophages that have been LFA-1 engaged and activated. Also, the neovascularization event (at least early) is anticipated to be driven by macrophages. The obvious difference in this model, however, is the inciting stimulus to macrophage recruitment. This model will study the macrophage response to ischemia, rather than chronic inflammation. Secondly, it has been demonstrated that ischemic tissue-localized macrophages play a significant role in the neovascular

response. A final approach to developing this new model is to assess a variety of pro-angiogenic, HuR dependent cytokines (in addition to VEGF) that are involved in the ischemic milieu. This will better help characterize the angiogenic picture before finally assessing vascularity via CD31+ immunohistochemistry staining.

In addition to establishing a new *in vivo* model, the nature of the macrophages in question will have to be better characterized. Several studies have recently described the plasticity and functional polarization of macrophages (60, 61, 62). Clasically, macrophage activation by IFN-ϒ, LPS, or TNF-α, is characterized by high capacity to present antigen, high production of reactive oxygen species, and high production of interleukin-12 (IL-12) and IL-23 (63). Functionally, they are potent effector cells, phagocytosing microorganisms, tumor cells, and producing proinflammatory cytokines. In the spectrum of macrophage polarization, these cells are referred to as M1 macrophages. An "alternative activation", initiated by a variety of alternative cytokines, produces M2 macrophages. These can be further subdivided based on the inducing agents: M2a (induced by IL-4, IL-13), M2b (induced by immune complexes and TLR agonists), and M2c (induced by IL-10 and glucocorticoid hormones) (64). M2 macrophages are characterized by low production of proinflammatory cytokines (IL-1, TNF-α, and IL-6) and functionally are involved in immunoregulation, tissue remodeling, and the promotion of angiogenesis. Therefore, the predominant cytokines within an inflammatory or ischemic milieu have the potential to polarize the macrophage, yielding very different functional outcomes.

When establishing subsequent *in vivo* models to assess the role of macrophages, it becomes critically important to understand the cytokine profile within the inflammatory

or ischemic environment. Furthermore, specific to our $HuR^{flox/flox}$LysMcre (KO) mouse, it is important to note if this genotype results in a significant polarization of the macrophage compared to it WT counterpart. A previous study has confirmed that human monocytes differentiated with GM-CSM or M-CSF have both M1 and M2 properties (63). Thus, the macrophages in the *in vitro* studies do not have a significant functional polarization and are likely to be homogeneous between WT and KO after a 7-day period of exposure to M-CSF. In addition to potential baseline genotypic differences, it will be of great interest to determine whether subsequent β2 integrin engagement confers a differentiation signal, in part through stabilization of a profile of otherwise labile transcripts. This may have significant implications on both our *in vitro* and *in vivo* model systems. Assessing the cytokine profile of HuR WT and KO macrophages before and after integrin engagement may be a reasonable study to address this hypothesis. These *in vitro* results may then be extrapolated to better understand the yet unknown cytokine profile of the hindlimb ischemia or PVA sponge implant model.

As our laboratory moves forward understanding the posttranscriptional regulation of mRNA transcripts in macrophages, we will continue to identify and characterize novel transcripts that are affected by β2 integrin engagement in a HuR dependent manner. The preliminary results for this endeavor have identified 300 genes in BMDMs upregulated upon engagement to ICAM-1. As for the HuR dependent genes, the findings were much smaller with only 29 apparent. The number of genes that were co-dependent on LFA-1 and HuR was only 5. Of note, this experiment was conducted prior to screening for HuR expression levels. As such, retrospective analysis confirmed a knockdown of HuR samples ranging from 59-96% knockdown, indicating significant variability amongst the

samples. Also, the genes known to be regulated by HuR (positive control genes) did not emerge from the analysis. Although this brings into question the validity of this microarray for assessing HuR dependent genes, further validation is warranted and will provide strong evidence in favor (or disfavor) of the current findings.

Through this study, we have shown that macrophage β2 integrin (LFA-1) engagement results in stabilization of the angiogenic transcript, VEGF mRNA, and that macrophage HuR is one of the components for mediating neovascular responses. As we move forward to alternative models of *in vivo* angiogenesis assays, we will broaden the scope of pro-angiogenic factors assessed in order to better characterize the angiogenic environment. Furthermore, the complex and plastic nature of recruited macrophages needs to be assessed in the setting of inflammation or ischemia. Our current findings, applied to our future directions, would provide an even deeper understanding of the post-transcriptional regulatory mechanisms of angiogenesis.

References

1. Hudlicka O, Brown M, Egginton S. Angiogenesis in skeletal and cardiac muscle. Physiol Rev 1992;72:369-417.

2. Habib G, Heibig J, Forman S, et al. Influence of coronary collateral vessels on myocardial infarct size in humans. Results of phase I thrombolysis in myocardial infarction (TIMI) trial. The TIMI Investigators. Circulation 1991;83:739-46.

3. Folkman J. Seminars in Medicine of the Beth Israel Hospital, Boston. Clinical applications of research on angiogenesis. N Engl J Med 1995;333:1757-63.

4. Folkman J. Diagnostic and therapeutic applications of angiogenesis research. C R Acad Sci III 1993;316:909-18.

5. Levy A, Levy N, Loscalzo J, et al. Regulation of vascular endothelial growth factor in cardiac myocytes. Circ Res 1995;76:758-66.

6. Lewis J, Lee J, Underwood J, Harris A, Lewis C. Macrophage responses to hypoxia: relevance to disease mechanisms. J Leukoc Biol 1999;66:889-900.

7. Levy A, Levy N, Goldberg M. Post-transcriptional regulation of vascular endothelial growth factor by hypoxia. J Biol Chem 1996;271:2746-53.

8. Penn J, Madan A, Caldwell R, Bartoli M, Caldwell R, Hartnett M. Vascular endothelial growth factor in eye disease. Prog Retin Eye Res 2008;27:331-71.

9. Ferrara N, Carver-Moore K, Chen H, et al. Heterozygous embryonic lethality induced by targeted inactivation of the VEGF gene. Nature 1996;380:439-42.

10. Plate K, Breier G, Weich H, Risau W. Vascular endothelial growth factor is a potential tumour angiogenesis factor in human gliomas in vivo. Nature 1992;359:845-8.

11. Aiello L, Avery R, Arrigg P, et al. Vascular endothelial growth factor in ocular fluid of patients with diabetic retinopathy and other retinal disorders. N Engl J Med 1994;331:1480-7.

12. Neufeld G, Cohen T, Gengrinovitch S, Poltorak Z. Vascular endothelial growth factor (VEGF) and its receptors. FASEB J 1999;13:9-22.

13. Dor Y, Porat R, Keshet E. Vascular endothelial growth factor and vascular adjustments to perturbations in oxygen homeostasis. Am J Physiol Cell Physiol 2001;280:C1367-74.

14. Schofield C, Ratcliffe P. Oxygen sensing by HIF hydroxylases. Nat Rev Mol Cell

Biol 2004;5:343-54.

15. Ikeda E, Achen M, Breier G, Risau W. Hypoxia-induced transcriptional activation and increased mRNA stability of vascular endothelial growth factor in C6 glioma cells. J Biol Chem 1995;270:19761-6.

16. Shima D, Kuroki M, Deutsch U, Ng Y, Adamis A, D'Amore P. The mouse gene for vascular endothelial growth factor. Genomic structure, definition of the transcriptional unit, and characterization of transcriptional and post-transcriptional regulatory sequences. J Biol Chem 1996;271:3877-83.

17. Forsythe J, Jiang B, Iyer N, et al. Activation of vascular endothelial growth factor gene transcription by hypoxia-inducible factor 1. Mol Cell Biol 1996;16:4604-13.

18. Brennan C, Steitz J. HuR and mRNA stability. Cell Mol Life Sci 2001;58:266-77.

19. Robinow S, Campos A, Yao K, White K. The elav gene product of Drosophila, required in neurons, has three RNP consensus motifs. Science 1988;242:1570-2.

20. Bornes S, Boulard M, Hieblot C, et al. Control of the vascular endothelial growth factor internal ribosome entry site (IRES) activity and translation initiation by alternatively spliced coding sequences. J Biol Chem 2004;279:18717-26.

21. Ozawa K, Kondo T, Hori O, et al. Expression of the oxygen-regulated protein ORP150 accelerates wound healing by modulating intracellular VEGF transport. J Clin Invest 2001;108:41-50.12.

22. Nathan C, Murray H, Cohn Z. The macrophage as an effector cell. N Engl J Med 1980;303:622-6.

23. Auger M. J., Ross J. A. The biology of the macrophage. In *The Macrophage* (C. E. Lewis and J. O'D. McGee. Eds.) Oxford, UK: Oxford University Press. 1993.

24. Cohn Z. Activation of mononuclear phagocytes: fact, fancy, and future. J Immunol 1978;121:813-6.

25. Gordon S. The Macrophage. Bioessays. 1995; 17:977-986.

26. Whitelaw D. The intravascular lifespan of monocytes. Blood 1966;28:455-64.

27. van Furth R. Origin and turnover of monocytes and macrophages. Curr Top Pathol 1989;79:125-50.

28. Hume D. The biology of macrophages. Sci Prog 1985;69:485-94.

29. Polverini P, Cotran P, Gimbrone MJ, Unanue E. Activated macrophages induce vascular proliferation. Nature 1977;269:804-6.

30. Janeway CA, Travers, P., Walport, m., and Shlomchik, M. J. Immunobiology: The Immune System in Health and Disease. New Yorj: Garland Publishing; 2001.

31. Rossetti G, Collinge M, Bender J, Molteni R, Pardi R. Integrin-dependent regulation of gene expression in leukocytes. Immunol Rev 2002;186:189-207.

32. Muller W, Randolph G. Migration of leukocytes across endothelium and beyond: molecules involved in the transmigration and fate of monocytes. J Leukoc Biol 1999;66:698-704.

33. Ledbetter J, June C, Grosmaire L, Rabinovitch P. Crosslinking of surface antigens causes mobilization of intracellular ionized calcium in T lymphocytes. Proc Natl Acad Sci U S A 1987;84:1384-8.

34. Wang G, Collinge M, Blasi F, Pardi R, Bender J. Posttranscriptional regulation of urokinase plasminogen activator receptor messenger RNA levels by leukocyte integrin engagement. Proc Natl Acad Sci U S A 1998;95:6296-301.

35. Pardi R, Bender J, Dettori C, Giannazza E, Engleman E. Heterogeneous distribution and transmembrane signaling properties of lymphocyte function-associated antigen (LFA-1) in human lymphocyte subsets. J Immunol 1989;143:3157-66.

36. Jaconi M, Theler J, Schlegel W, Appel R, Wright S, Lew P. Multiple elevations of cytosolic-free Ca2+ in human neutrophils: initiation by adherence receptors of the integrin family. J Cell Biol 1991;112:1249-57.

37. Kanner S, Grosmaire L, Ledbetter J, Damle N. Beta 2-integrin LFA-1 signaling through phospholipase C-gamma 1 activation. Proc Natl Acad Sci U S A 1993;90:7099-103.

38. Fällman M, Gullberg M, Hellberg C, Andersson T. Complement receptor-mediated phagocytosis is associated with accumulation of phosphatidylcholine-derived diglyceride in human neutrophils. Involvement of phospholipase D and direct evidence for a positive feedback signal of protein kinase. J Biol Chem 1992;267:2656-63.

39. Stoecklin G, Hahn S, Moroni C. Functional hierarchy of AUUUA motifs in mediating rapid interleukin-3 mRNA decay. J Biol Chem 1994;269:28591-7.

40. Shaw G, Kamen R. A conserved AU sequence from the 3' untranslated region of GM-CSF mRNA mediates selective mRNA degradation. Cell 1986;46:659-67.

41. Lagnado C, Brown C, Goodall G. AUUUA is not sufficient to promote poly(A) shortening and degradation of an mRNA: the functional sequence within AU-rich elements may be UUAUUUA(U/A)(U/A). Mol Cell Biol 1994;14:7984-95.

42. Zubiaga A, Belasco J, Greenberg M. The nonamer UUAUUUAUU is the key AU-rich sequence motif that mediates mRNA degradation. Mol Cell Biol 1995;15:2219-30.

43. Wilson G, Lu J, Sutphen K, Sun Y, Huynh Y, Brewer G. Regulation of A + U-rich element-directed mRNA turnover involving reversible phosphorylation of AUF1. J Biol Chem 2003;278:33029-38.

44. Gherzi R, Lee K, Briata P, et al. A KH domain RNA binding protein, KSRP, promotes ARE-directed mRNA turnover by recruiting the degradation machinery. Mol Cell 2004;14:571-83.

45. Fan X, Steitz J. Overexpression of HuR, a nuclear-cytoplasmic shuttling protein, increases the in vivo stability of ARE-containing mRNAs. EMBO J 1998;17:3448-60.

46. Wang J, Collinge M, Ramgolam V, et al. LFA-1-dependent HuR nuclear export and cytokine mRNA stabilization in T cell activation. J Immunol 2006;176:2105-2113.

47. Zhang X, Goncalves R, Mosser D. The isolation and characterization of murine macrophages. Curr Protoc Immunol 2008;Chapter 14:Unit 14.1.

48. Valdramidou D, Humphries, Martin J., Mould, Paul A. Distinct Roles of β1 Metal Ion-dependent Adhesion Site (MIDAS), Adjacent to MIDAS (ADMIDAS), and Ligand-associated Metal-binding Site (LIMBS) Cation-binding Sites in Ligand Recognition by Integrin 2β1. In: J. Biol Chem.; 2008:32704-14.

49. Capecchi M. The new mouse genetics: altering the genome by gene targeting. Trends Genet 1989;5:70-6.

50. Thomas K, Capecchi M. Site-directed mutagenesis by gene targeting in mouse embryo-derived stem cells. Cell 1987;51:503-12.

51. Clausen B, Burkhardt C, Reith W, Renkawitz R, Förster I. Conditional gene targeting in macrophages and granulocytes using LysMcre mice. Transgenic Res 1999;8:265-77.

52. Kyriakides T, Zhu Y, Yang Z, Huynh G, Bornstein P. Altered extracellular matrix remodeling and angiogenesis in sponge granulomas of thrombospondin 2-null mice. Am J Pathol 2001;159:1255-62.

53. Ammerpohl O, Schmitz A, Steinm ller L, Renkawitz R. Repression of the mouse M-lysozyme gene involves both hindrance of enhancer factor binding to the methylated enhancer and histone deacetylation. Nucleic Acids Res 1998;26:5256-60.

54. Ramos-DeSimone N, Hahn-Dantona E, Sipley J, Nagase H, French D, Quigley J. Activation of matrix metalloproteinase-9 (MMP-9) via a converging plasmin/stromelysin-1 cascade enhances tumor cell invasion. J Biol Chem 1999;274:13066-76.

55. Tressel S, Huang R, Tomsen N, Jo H. Laminar shear inhibits tubule formation and migration of endothelial cells by an angiopoietin-2 dependent mechanism. Arterioscler Thromb Vasc Biol 2007;27:2150-6.

56. Shweiki D, Itin A, Soffer D, Keshet E. Vascular endothelial growth factor induced by hypoxia may mediate hypoxia-initiated angiogenesis. Nature 1992;359:843-5.

57. Bucala R, Spiegel L, Chesney J, Hogan M, Cerami A. Circulating fibrocytes define a new leukocyte subpopulation that mediates tissue repair. Mol Med 1994;1:71-81.

58. Hartlapp I, Abe R, Saeed R, et al. Fibrocytes induce an angiogenic phenotype in cultured endothelial cells and promote angiogenesis in vivo. FASEB J 2001;15:2215-24.

59. Goto T, Fukuyama N, Aki A, Kanabuchi K, Mori H, Inoue H. Search for appropriate experimental methods to create stable hind-limb ischemia in mouse. In: J Exp Clin Med.; 2006:128-32.

60. Gordon S. Alternative activation of macrophages. Nat Rev Immunol 2003;3:23-35.

61. Mosser D. The many faces of macrophage activation. J Leukoc Biol 2003;73:209-12.

62. Mantovani A, Sozzani S, Locati M, Allavena P, Sica A. Macrophage polarization: tumor-associated macrophages as a paradigm for polarized M2 mononuclear phagocytes. Trends Immunol 2002;23:549-55.

63. Verreck F, de Boer T, Langenberg D, et al. Human IL-23-producing type 1 macrophages promote but IL-10-producing type 2 macrophages subvert immunity to (myco)bacteria. Proc Natl Acad Sci U S A 2004;101:4560-5.

64. Mantovani A, Sica A, Sozzani S, Allavena P, Vecchi A, Locati M. The chemokine system in diverse forms of macrophage activation and polarization.

Trends Immunol 2004;25:677-86.

Figure 1: Phenotype of murine BMDMs. Murine bone marrow derived macrophages were isolated and cultured as described in the Methods section in RPMI media supplemented with M-CSF. After 7 days of culture, adherent cells were harvested to assess the purity of the macrophage population. The samples were analyzed by flow cytometry and double stained with FITC-conjugated anti-F4/80 antibody and PE-conjugated anti-CD11b antibody (both identifying markers of macrophages).

Figure 2: Effect of LFA-1 engagement on VEGF mRNA decay. After 7 days of bone marrow derived isolation and expansion (see Methods section), cells were harvested, washed in LFA-1 activation buffer (cation-based solution) and adhered to ICAM-1 or FC conjugate control plates for 30 minutes before being replaced with RPMI for an additional 2.5 hours. At 3 hours, a transcriptional inhibitor DRB was added (time 0). The RNA was harvested at time 0, 30, and 60 minutes for VEGF real-time. VEGF mRNA levels were normalized to GAPDH mRNA levels. (N = 3, mean +/- SD).

Figure 3: β2 integrin-induced HuR translocation in BMDMs. After 7 days of proliferation in RPMI/L Cell enriched media, BMDMs were harvested and suspended in LFA-1 activation buffer (cation-based solution), following which they were plated on coverslips coated with immobilized recombinant ICAM-1 or FC conjugate control for 45 minutes. Cells were then fixed (4 % paraformaldehyde) and permeabilized (0.1% Triton X-100). Immunofluorescent analysis was performed with anti-HuR antibody (red) and the nuclear marker DAPI (blue). Magnification of the images is 1000x. These results are representative of 4 independent experiments.

Figure 4: β2 integrin-induced p38 MAPK activation in BMDMs. Murine BMDMs were harvested after 7 days of proliferation and differentiation in RPMI/L Cell enriched media. Cells were suspended in LFA-1 activation buffer and plated on ICAM-1 coated plates or control plates for 5, 10, 15, and 25 minutes. Non-adherent cells were aspirated and adherent cells were collected and lysed at the respective time points. The cell lysates were immunoblotted for phosphorylated p38 MAPK and total p38. "No Tx" lane indicates lysates from non-adherent cells (serving as a secondary negative control). Lanes "L5" to "L25" represent lysates from adherent control samples and lanes "I5" to "I25" represent lysate samples from cells adherent to ICAM-1. Phosphorylated p38 was normalized to total p38 MAPK. These results are representative of 3 independent experiments.

Figure 5: Targeting the Elavl1 (Hu antigen R) gene.

Figure 6: HuR levels in macrophage-specific HuR KO cells. BMDMs and splenic lymphocytes were isolated from $HuR^{flox/flox}$ and $HuR^{flox/flox}$LysMcre mice. After isolation of BMDMs, cells underwent a 7 day culture process in RPMI + L cell enriched media. Lymphocytes were purified from the splenocyte population using a Histopaque gradient.

Purified cells populations were then lysed and immunoblotted for HuR AUF-1 (serving as a non-gene manipulated RNA binding protein control).

Figure 7: HuR expression in WT and KO BMDMs. Bone marrow derived macrophages were isolated from 3 $HuR^{flox/flox}$ and 3 $HuR^{flox/flox}$LysMcre mice from different littermates. After isolation of BMDMs, cells underwent a 7 day proliferation and differentiation in RPMI + L cell enriched media. Cells were then harvested, lysed, and extracts immunoblotted for HuR and actin as a control for normalization.

Figure 8: HuR expression levels from WT and KO BMDMs. Bone marrow derived macrophages were isolated from 3 $HuR^{flox/flox}$ and 3 $HuR^{flox/flox}$LysMcre mice from different littermates. After isolation of BMDMs, cells underwent a 7 day proliferation and differentiation in RPMI + L cell enriched media. Cells were then harvested, lysed, and RNA extracted for reverse transcription and real-time PCR for HuR. Data are displayed as % of mRNA levels of WT controls (e.g. KO 1 HuR mRNA % of WT 1).

Figure 9: FACS analysis of HuR expression in WT and KO macrophages. Murine bone marrow derived macrophages were isolated and cultured as described in the Methods section in RPMI media supplemented with M-CSF. After 7 days of culture, adherent cells were harvested for flow cytometric analysis. The BMDMs from WT and KO mice were stained with an Alexa-648 conjugated anti-F4/80 antibody and a PE-conjugated anti-CD11b antibody. Cells were subsequently permeabilized and stained with anti-HuR antibody conjugated to a zenon alexa 488 tag or corresponding isotype control. Cells were first gated on the live population and then gated on the double positive F4/80, CD11b population to analyze macrophages only. Within this gated population, HuR expression levels from WT and KO samples stained with anti-HuR or the isotype control are shown. A table comparing geometric means of the histograms is shown on the right.

Figure 10: Phenotype of HuR+ cells in the KO population. As in figure 8, differentiated BMDMS from KO mice were stained with an Alexa-648 conjugated anti-F4/80 antibody and a PE-conjugated anti-CD11b antibody. Cells were subsequently permeabilized and stained with anti-HuR antibody conjugated to a zenon alexa 488 tag or corresponding isotype control. In order to confirm the presence of HuR in the CD11b+, F4/80+ cell population, a technique of "back-gating" was used. When gating only the HuR positive cells from the KO sample (difference between KO HuR and KO isotype histogram), this subpopulation of cells can be assessed for CD11b, F4/80 macrophage markers.

Figure 11: HuR FACS analysis in mouse peripheral blood leukocyte subsets. Peripheral blood was acquired via retrobulbar bleeding from WT and KO mice. RBC lysis was performed and remaining leukocytes were surface stained with Alexa-648

conjugated anti-F4/80 antibody and a PE-conjugated anti-CD11b antibody. Cells were subsequently permeabilized and stained with anti-HuR antibody conjugated to a zenon alexa 488 tag or corresponding isotype control. After live gating, were gated as double positive (F4/80+, CD11b+) in order to identify macrophages or single positive (F4/80-, CD11b+) in order to identify granulocytes (and NK cells). HuR expression levels within these gated populations were then assessed.

Figure 12: Loss of Integrin-induced VEGF mRNA stabilization in HuR KO BMDMs. After 7 days of bone marrow derived isolation and expansion from WT and KO mice (see Methods), cells were harvested, washed in LFA-1 activation buffer and adhered to immobilized recombinant ICAM-1 plates for 30 minutes followed by replacement with complete media for an additional 2.5 hours.. At 3 hours, DRB was added (time 0). The RNA from WT and KO BMDMs was harvested at time 0, 30, and 60 minutes for real-time, VEGF RT-PCR. VEGF mRNA levels were normalized to GAPDH mRNA levels. (N = 2, mean +/- SD).

Figure 13: VEGF protein levels in supernatants recovered from integrin-engaged WT and KO BMDMs. After 7 days of bone marrow derived isolation and expansion from WT and KO mice (see Methods), cells were harvested, washed in LFA-1 activation buffer and adhered to immobilized recombinant ICAM-1 plates or Fc conjugate control plates for 30 minutes, followed by replacement with complete media for 23 hours. The supernatant was then collected and VEGF protein levels were determined by ELISA. (N = 2, mean +/- SD).

Figure 14: VEGF mRNA expression levels from PVA sponge implants. Sterile polyvinyl alcohol sponges were inserted into the dorsum of WT and KO mice. At indicated time points (3 days, 1, 2, 3, and 4 weeks), the mice were euthanized and the sponges were explanted. For RNA isolation, the skin was detached from the sponge. The sponge was then minced and homongenized using a tissue homogenizer in RLT lysis buffer. RNA was isolated via a RNeasy kit (Qiagen) followed by reverse transcription, and analyzed via real-time PCR. Murine VEGF mRNA levels were normalized to GAPDH mRNA at each time point. Expression levels are illustrated as a fold increase over the "3 D KO" (three day knockout) sponge VEGF mRNA level. Note: 3 pooled mice were used to achieve adequate total RNA concentration.

Figure 15: FACS quantification of macrophages in explanted PVA sponges. PVA sponges were implanted subcutaneously over the dorsum of WT and KO mice. Sponges were explanted at 2, 3, and 4 weeks post-implantation and cells were extracted via Collagenase Type I digestion. RBCs were subsequently lysed and remaining cells were manually counted. Cells were then surface stained with Alexa-648 conjugated anti-F4/80 antibody and a PE-conjugated anti-CD11b antibody. After live gating, cells from 3 and 4

week PVA sponge implants were analyzed for F4/80 plus CD11b positivity (figure on left). Combining the absolute cell counts and the % of double-positive cells, the total number of macrophages infiltrating the sponge were calculated (figure on right).

Figure 16: CD31+ microvessels in implanted PVA sponges (4 wks). PVA sponges were implanted subcutaneously over the dorsum of WT and KO mice. Sponges and adherent skin were explanted at 2, 3, and 4 weeks post-implantation and fixed overnight in a formalin-free zinc fixative solution, embedded in paraffin, and sectioned into 5 µm sections. Immunohistochemistry staining using anti-CD31 antibody was performed (secondary: biotinylated anti-rat). CD31 positivity is illustrated in the 4 wk wild type mouse at both low and high magnification.

Figure 17: Neovessel quantification in PVA sponges implanted in macrophage HuR WT and KO mice. PVA sponges were implanted subcutaneously over the dorsum of WT and KO mice. Sponges and adherent skin were explanted at 2, 3, and 4 weeks post-implantation and fixed overnight in a formalin-free zinc fixative solution, embedded in paraffin, and sectioned into 5 µm sections. Immunohistochemistry staining using anti-CD31 antibody was performed. CD31 positivity in 2 week and 4 week WT and KO sponges are illustrated in 17A, as well as in 3 week and 4 week blinded individuals in 17B. All vessels were manually counted by two blinded individuals. 17A represents an average of CD31+ vessels in 25 fields of view under high magnification, while 17B represents all the CD31+ vessels present in each sponge. Numbers represent an average of two counts.

Figure 18: RT-PCR validation of microarray diff score data. Microarray analysis comparing gene expression levels in BMDMs isolated from $HuR^{flox/flox}$(WT) and $HuR^{flox/flox}$LysMcre (KO) mice, bound or unbound to ICAM-1 was performed using Illumina's Beadstudio software program. To analyze the HuR-independent components of the microarray, the reference group was set to "WT No Tx" (no treatment). The filter, a simple AND/OR algorithm was set as follows: Branch 1 = KO, diff score >13, KO, diff score < -13. Branch 2 = KO, *p*-value < 0.01, WT No Tx, *p*-value < 0.01. This analysis resulted in 5924 genes with ~ 300 genes having + Diff scores comparing WT ICAM bound to the reference group. Within this group of 300, several chemokine genes had significant induction patterns on ICAM-1. These chemokines were selected for validation via RT-PCR. Primers were designed for CCL2, CCL3, CCL4, CCL5, and CCL7. An identical experiment was conducted using BMDMs from a WT and KO mouse. On the left, the original microarray Diff scores are demonstrated. On the right, the validated RT-PCR data demonstrates transcript expression levels normalized to GAPDH.

Table/Figure 19: Integrin and HuR-dependent gene expression levels from WT and KO macrophages. Microarray analysis comparing gene expression levels in BMDMs isolated from $HuR^{flox/flox}$(WT) and $HuR^{flox/flox}$LysMcre (KO) mice, bound or unbound to ICAM-1, was performed. To analyze the HuR-dependent components of the microarray, the reference group was set to "KO 3" (ICAM engaged). The filter, a simple AND/OR algorithm was set as follows: Branch 1 = WT 3, diff score >13, WT 3, diff score < -13. Branch 2 = WT 3, *p*-value < 0.01, KO 3, *p*-value < 0.01. This analysis resulted in 1045 genes with 29 genes having + Diff scores comparing WT 3 with the reference group, KO 3. Table 1 lists all the genes that show a statistically significant difference between WT 3 (ICAM-bound) and KO 3 (ICAM-bound) groups. Genes are listed by descending dif scores for WT 3. The "comments" column in the table identifies 5 genes that have both HuR-dependent and LFA-1 dependent expression patterns. The average signal intensities of these five genes from the original microarray are illustrated in Figure 19.

Figure 1 ***Phenotype of murine BMDMs***

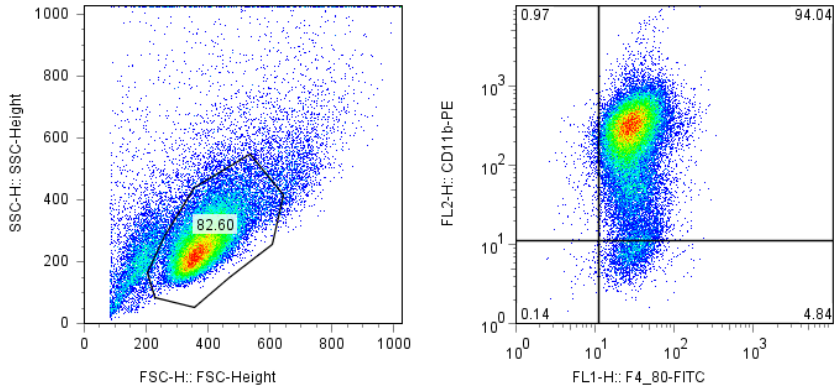

Figure 2 ***Effect of LFA-1 engagement on VEGF mRNA decay***

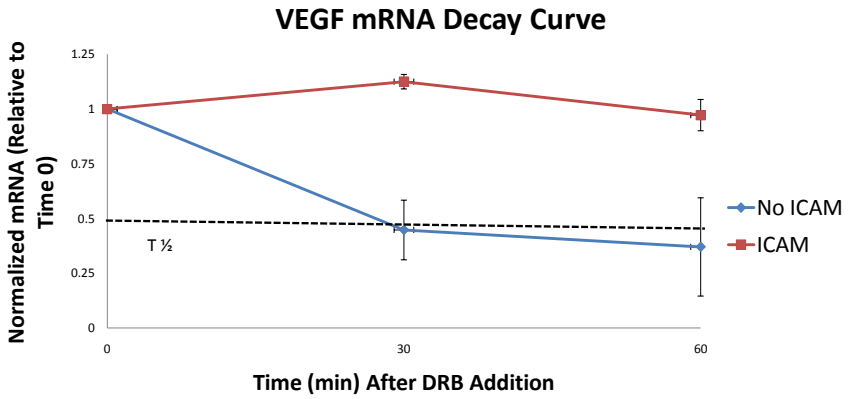

Figure 3 ***β2 integrin-induced HuR translocation in BMDMs***

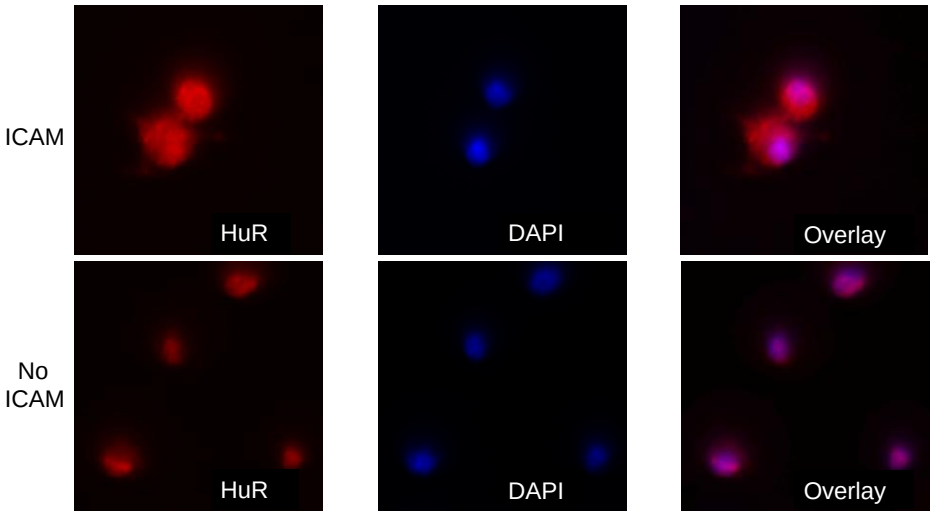

Figure 4 ***β2 integrin-induced p38 MAPK activation in BMDMs***

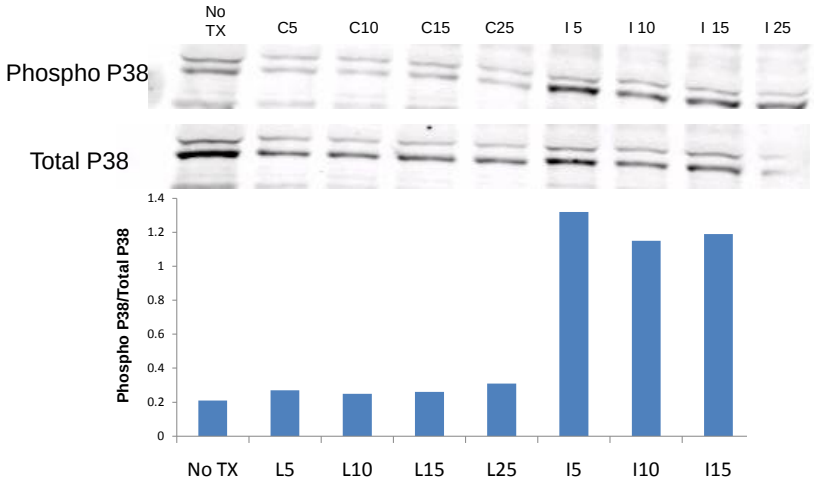

Figure 5 ***Targeting the Elavl1 (HuR) gene***

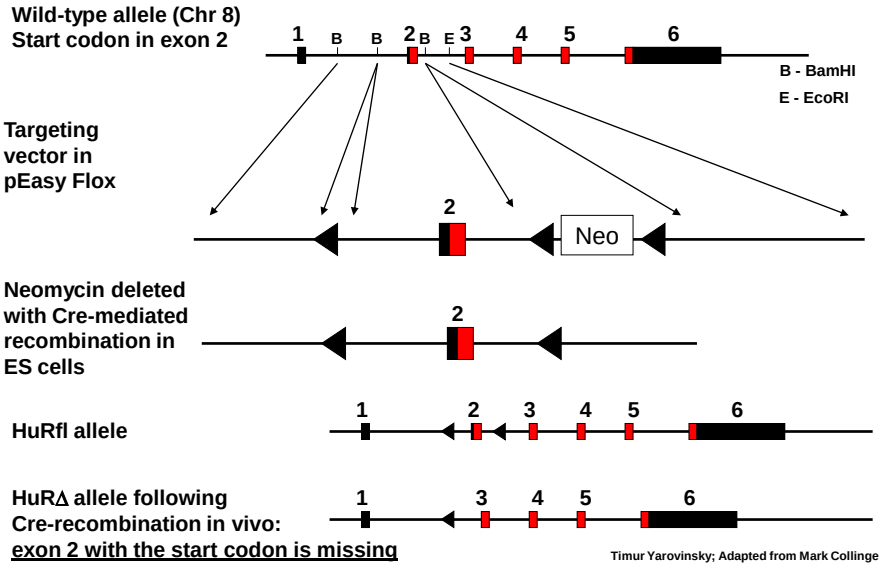

Figure 6 ***HuR levels in macrophage-specific HuR KO cells***

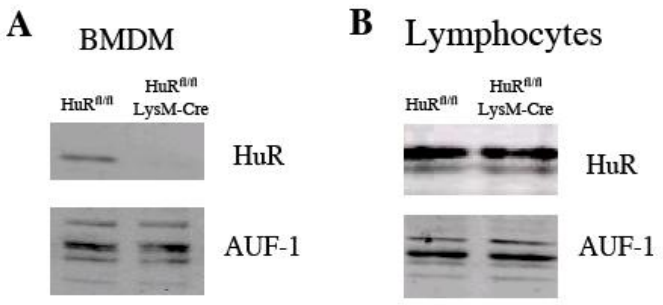

Figure courtesy of Mark Collinge

Figure 7 ***HuR Expression in WT and KO BMDMs***

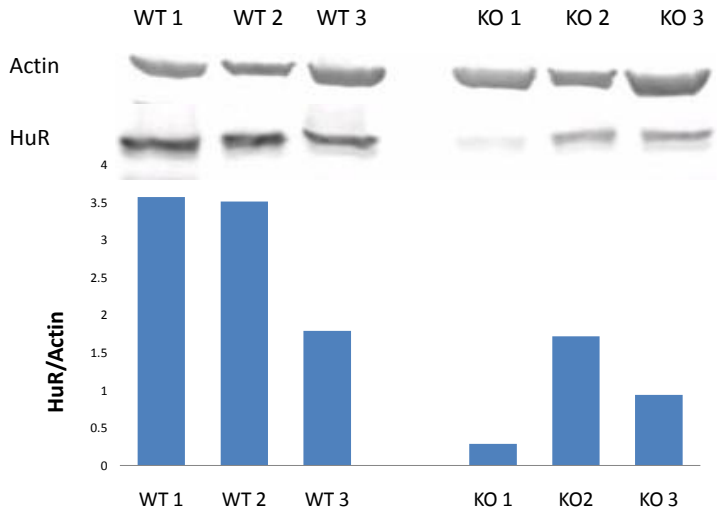

Figure 8 ***HuR mRNA expression levels from WT and KO BMDMs***

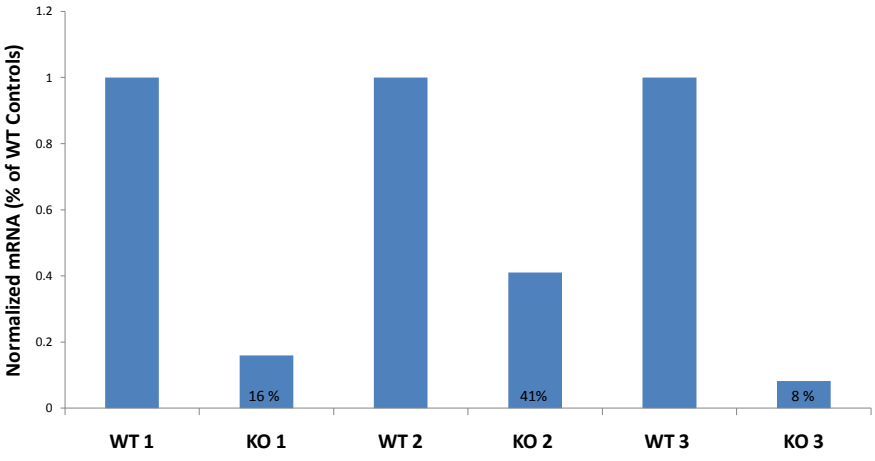

Figure 9 ***FACS analysis of HuR expression in WT and KO macrophages***

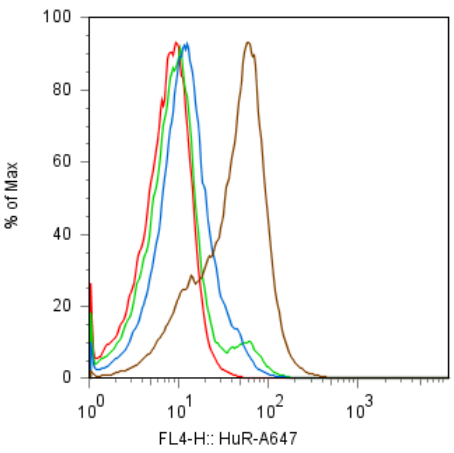

Sample Name	Geom. Mean , FL4-H
WT-F480,CD11b,,HuR.001	36.90
KO-F480,CD11b,,HuR.002	11.11
WT-F480,CD11b,,iso.003	8.91
KO-F480,CD11b,,iso.004	6.89

Figure 10 ***Phenotype of HuR+ cells in the KO population***

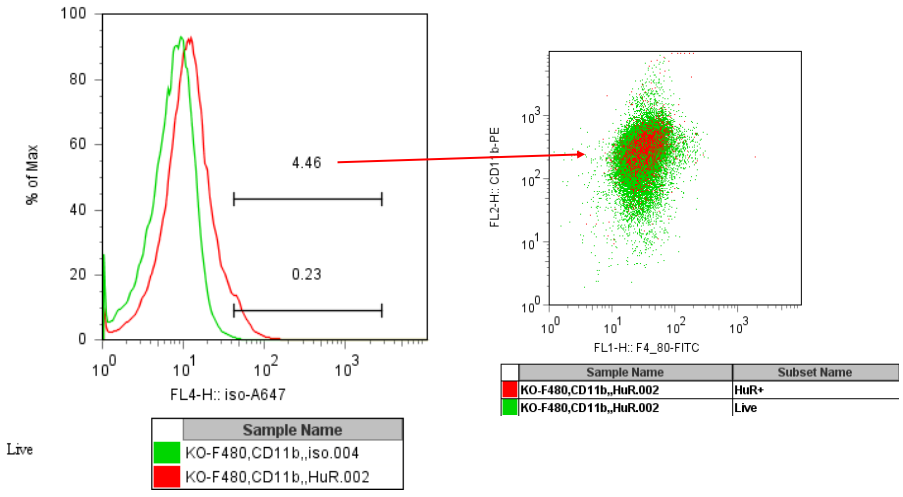

Sample Name	Subset Name
KO-F480,CD11b,,HuR.002	HuR+
KO-F480,CD11b,,HuR.002	Live

Figure 11 ***HuR FACS analysis on mouse peripheral blood leukocyte subsets***

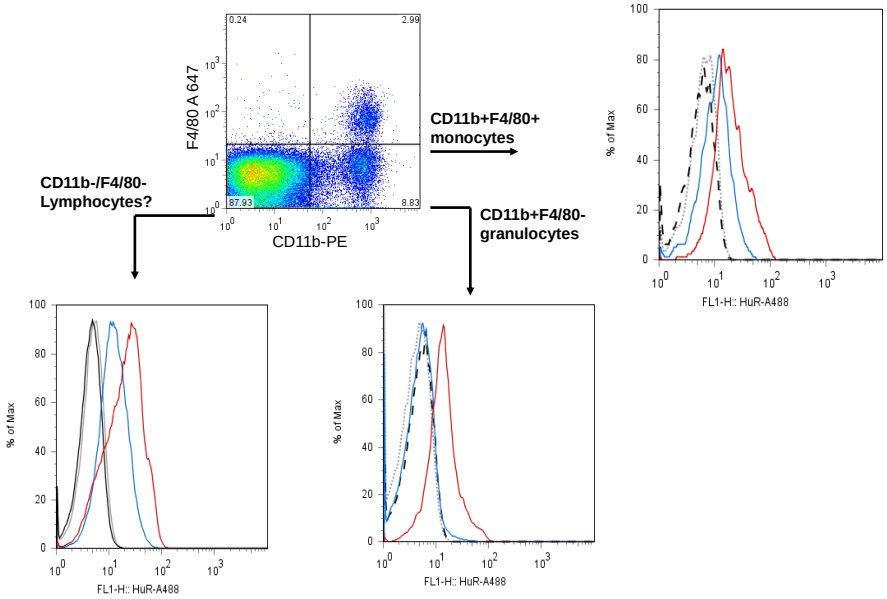

Figure 12 ***Loss of integrin-induced VEGF mRNA stabilization in HuR KO BMDMs***

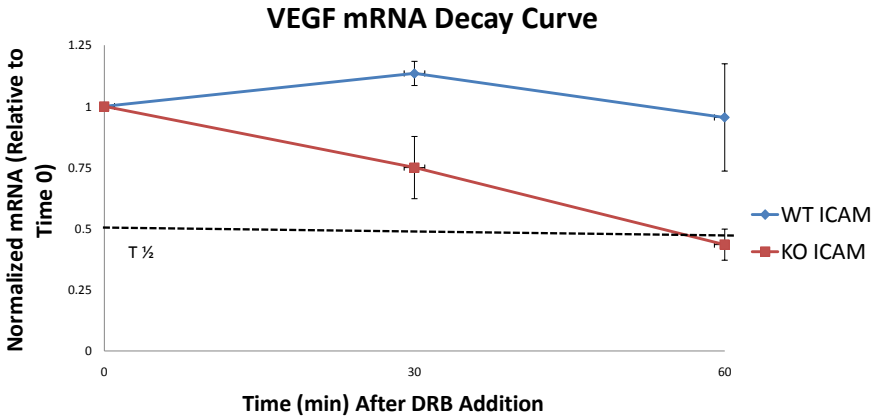

Figure 13 ***VEGF protein levels in supernatants recovered from integrin-engaged WT and KO BMDMs***

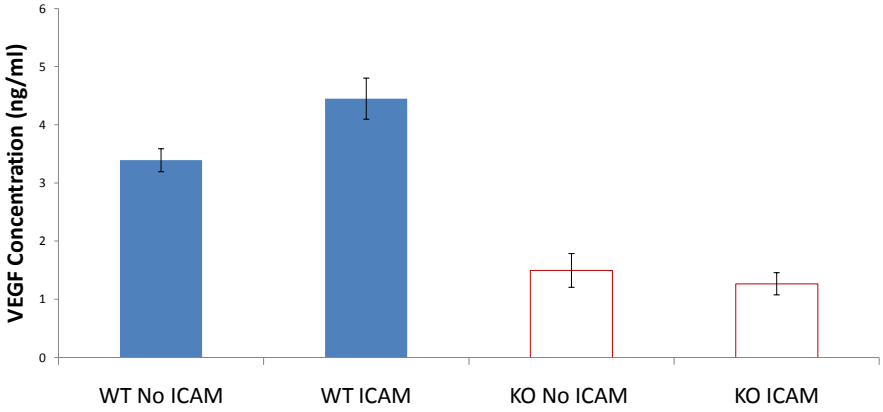

Figure 14 ***VEGF mRNA expression levels from PVA sponge implants***

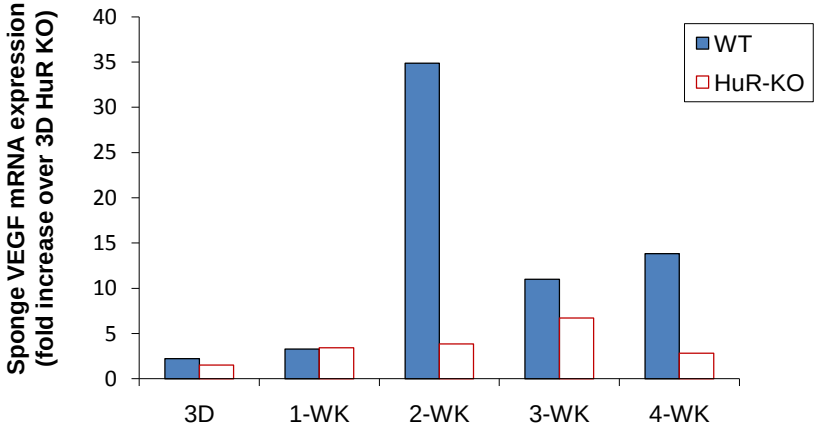

Figure 15 ***FACS quantification of macrophages in explanted PVA sponges***

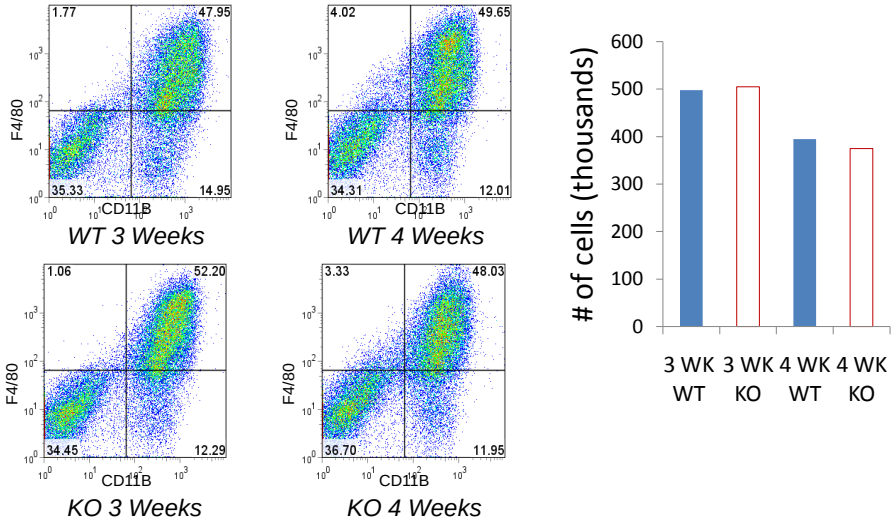

Figure 16 ***CD31+ microvessels in implanted PVA sponges (4 wk)***

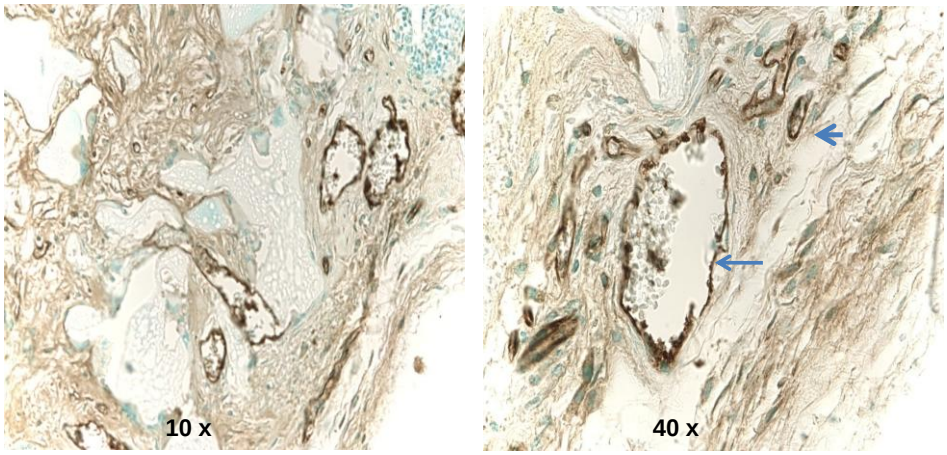

Figures 17A, 17B ***Neovessel quantification in PVA sponges implanted in macrophage HuR WT and KO mice***

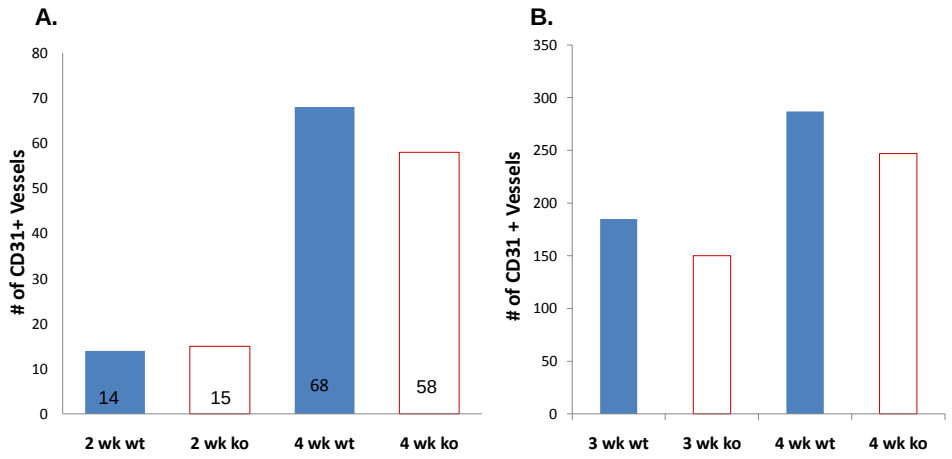

Figure 18 ***RT-PCR validation of microarray Diff score data***

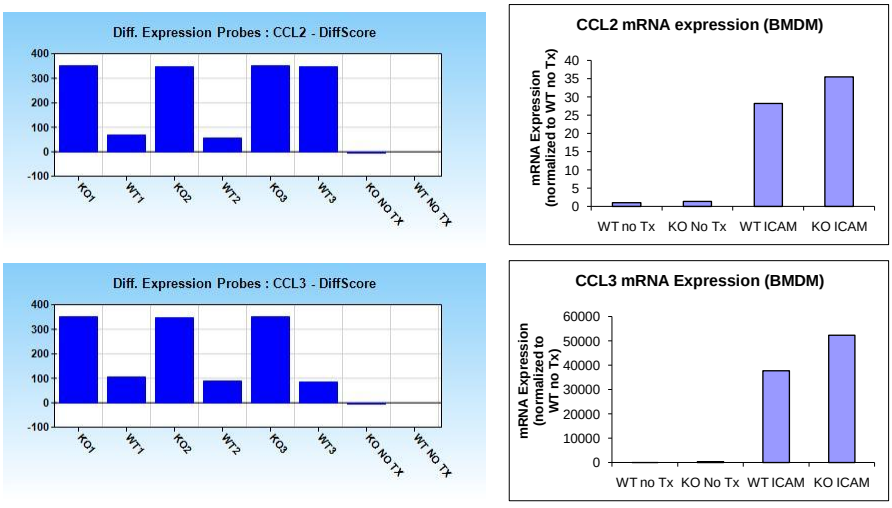

Figure 18 ***RT-PCR validation of microarray Diff score data***

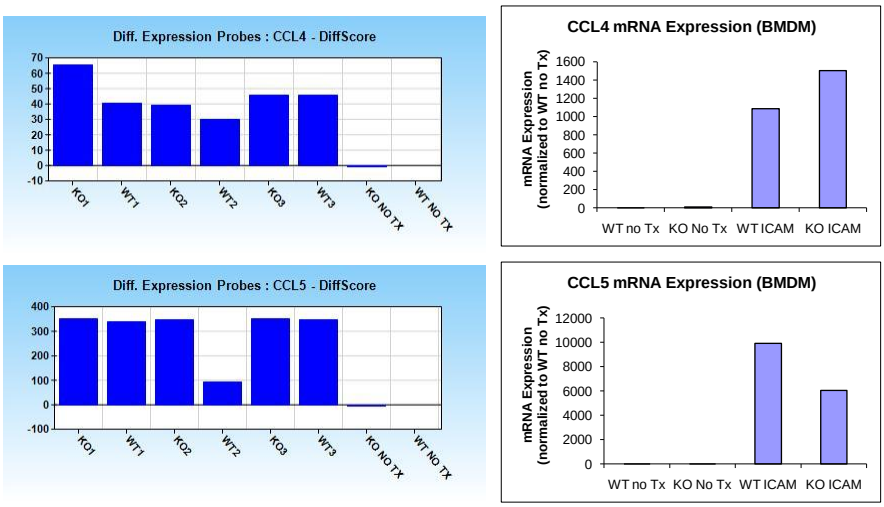

Figure 18 ***RT-PCR validation of microarray Diff score data***

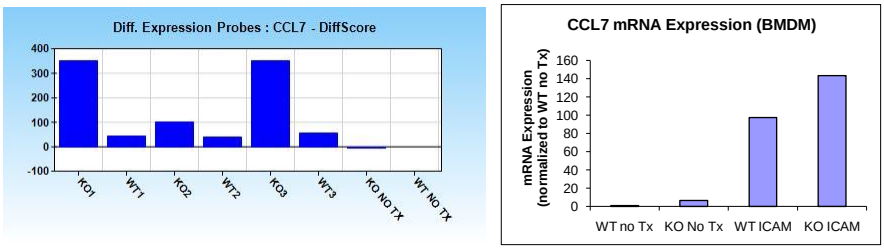

Figure 19 **Integrin and HuR-dependent gene expression levels from WT and KO macrophages**

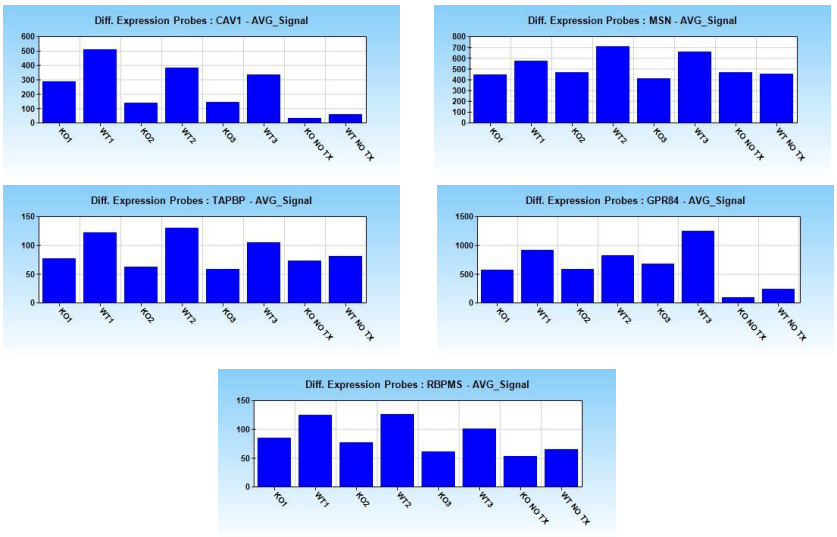

Table: Microarray Transcript Data: ICAM and/or HuR Dependence (Diff score > + 13)

Gene Symbol	***Gene Name***	***Comments***
Cav1	Caveolin 1	HuR/LFA-1
XIST	inactive X specific transcripts	
EIF2S3X	eukaryotic translation initiation factor 2, subunit 3, structural gene X-linked	
TAPBP	TAP Binding Protein	HuR/LFA-1
MSN	Moesin	HuR/LFA-1
LysS	Lysozyme S	
THOC4	THO complex 4	
GNB1	guanine nucleotide binding protein (G protein), beta 1	
TFRC	transferrin receptor (p90, CD71)	
PDIA6	protein disulfide isomerase associated 6	
CCNB1	cyclin B1	
PRDX1	peroxiredoxin 1	
RAC1	RAS-related C3 botulinum substrate 1	
GPR84	G protein-coupled receptor 84	HuR/LFA-1
MS4A6D	membrane-spanning 4-domains, subfamily A, member 6D	
KCMF1	potassium channel modulatory factor 1	
SLC39A4	solute carrier family 39 (zinc transporter), member 4	
CD276	CD276 antigen	
PPIC	peptidyl-prolyl cis-trans isomerase C	
TRP53INP2	transformation related protein 53 inducible nuclear protein 2	
LPCAT2	lysophosphatidylcholine acyltransferase 2	
MTCH2	mitochondrial carrier homolog 2	
PSMA7	proteasome (prosome, macropain) subunit, alpha type 7	
RBPMS	RNA binding protein gene with multiple splicing	HuR/LFA-1
SRPK1	serine/arginine-rich protein specific kinase 1	
COPZ2	coatomer protein complex, subunit zeta 2	
PPAPDC1	phosphatidic acid phosphatase type 2 domain containing 1B	
PSMG2	proteasome (prosome, macropain) assembly chaperone 2	
EBPL	emopamil binding protein-like	